Cambridge Materials: Energy (2026), **1**, e3, 1–30
doi:10.1017/S2978169826000021

CAMBRIDGE UNIVERSITY PRESS

Review

Molecular engineering of polystyrene: Catalytic deconstruction, precise functionalization, and material transformation

Haiyang Song‡, Xiangjin Zhang‡ and Xuefeng Jiang
East China Normal University, China

Abstract

The highly stable carbon–carbon backbone of polystyrene (PS) leads to severe environmental accumulation. To overcome the polymer deterioration and low economic value associated with traditional mechanical recycling and pyrolysis, the molecular-level conversion of waste PS into high-value chemicals and advanced materials is recognized as a critical pathway. This review categorizes the chemical upcycling of PS into two main pathways: "Breaking the Backbone" (destructive cleavage) and "re-using the skeleton" (non-destructive editing). While systematically summarizing multi-energy-driven (e.g., thermal, photochemical, and electrical) deconstruction strategies that cleave the inert C(sp^3)–C(sp^3) main chain, this review also examines site-selective C(sp^2)–H post-polymerization modification. By introducing functional groups onto the intact polymer skeleton, waste PS is converted into value-added materials. Preliminary life-cycle assessments (LCA) indicate that preserving the skeleton mitigates the energy penalty of complete backbone cleavage, offering a pragmatic and low-carbon route for plastics recycling.

Impact Statement

The non-degradable carbon–carbon backbone of polystyrene (PS) has caused severe environmental accumulation, demanding a paradigm shift from energy-intensive incineration or low-value downcycling to molecular-level upcycling. This review presents a molecular engineering framework that strategically divides PS upcycling into two complementary pathways: breaking the backbone via multi-energy-driven catalysis (thermal, photochemical, electrochemical) to recover monomers and fuels, and re-using the skeleton through site-selective C–H functionalization that preserves the polymer architecture while introducing valuable chemical handles. Critically, our sustainability-centric analysis challenges idealized laboratory assumptions by revealing that complete backbone cleavage incurs prohibitive energy and feedstock logistics costs, whereas skeletal preservation offers a low-carbon, carbon-retentive alternative yet requires robust management of real-world impurities. By integrating life-cycle and techno-economic assessments, we establish a decision-making framework that matches feedstock quality with product value. Successful scaling demands simultaneous innovations in catalyst poisoning resistance, solvent-free processing, and biochemical hybrid cascades, ultimately providing a viable blueprint for a circular plastics economy that reconciles environmental restoration with economic competitiveness.

Keywords: Chemical upcycling; Plastics circular economy; Polystyrene; Precise functionalization

(Received: 14 August 2026; revised: 27 August 2026; accepted: 31 August 2026)

1. Introduction

As one of the most widely used aromatic thermoplastics globally, polystyrene (PS) is extensively applied in packaging, construction materials, electronic devices, and daily consumer goods (Figure 1) [1–4]. However, its degradation in natural environments is severely hindered by its highly stable carbon–carbon backbone and inert hydrophobic skeleton. To comprehensively contextualize the imperative for advanced recycling, the macroscopic landscape of plastic waste management must be critically examined (Figure 2). Traditional end-of-life trajectories, including widespread landfilling and quaternary recycling via incineration, not only exacerbate severe environmental burdens but also result in the complete annihilation of the embedded petrochemical value. Meanwhile, primary and secondary mechanical recycling pathways typically involve physically shredding and grinding bulky PS wastes into flakes or powders to circumvent immediate disposal. [5–13] However, these rudimentary processes destroy the material's macroscopic integrity, relegating the crushed plastics to serve merely as low-value inert fillers in construction or agriculture. This inevitable polymer performance deterioration and "downcycling" perfectly underscore the imperative for molecular-level valorization [14–26].

Consequently, according to official standard classifications (ISO 15270 and ASTM D7209), tertiary recycling—commonly termed chemical recycling—has emerged as the most scientifically and economically viable paradigm to break this linear disposal model

‡These authors contributed equally
Corresponding author: Xuefeng Jiang; Email: xfjiang@chem.ecnu.edu.cn
Cite this article: H. Song, X. Zhang and X. Jiang. 'Molecular engineering of polystyrene: Catalytic deconstruction, precise functionalization, and material transformation'. *Cambridge Materials: Energy*, **1**, e3: (2026), 1–30.
https://doi.org/10.1017/S2978169826000021

© The Author(s), 2026. Published by Cambridge University Press. This is an Open Access article, distributed under the terms of the Creative Commons Attribution licence (http://creativecommons.org/licenses/by/4.0), which permits unrestricted re-use, distribution and reproduction, provided the original article is properly cited.

Downloaded from https://www.cambridge.org/core. 15 Nov 2026 at 12:57:10, subject to the Cambridge Core terms of use.

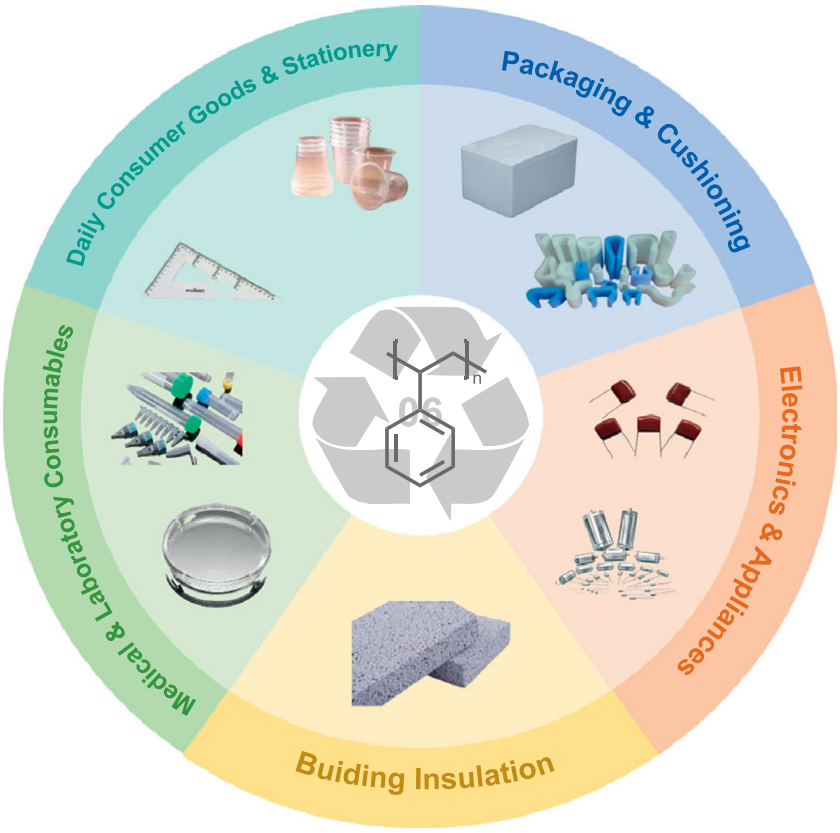


Figure 1. Multifunctional applications on PS.

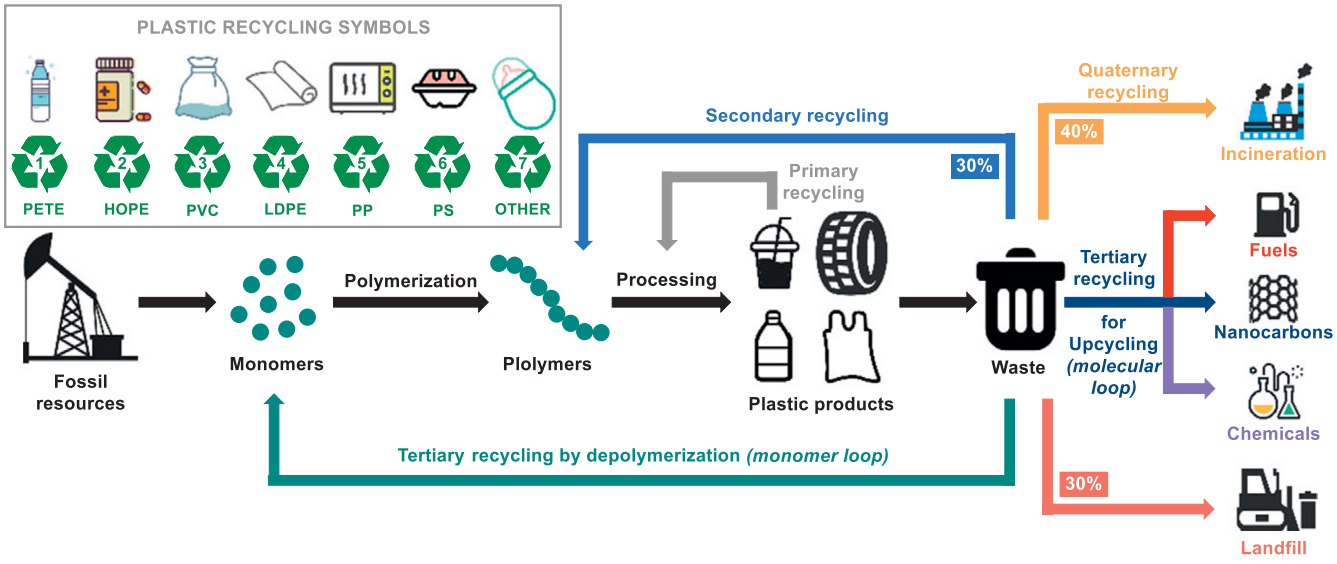


Figure 2. Life cycle of polymeric materials and main recycling technologies.

[27–30]. As illustrated, this approach bifurcates into the "monomer loop" (depolymerization to recover virgin monomers) and the advanced "molecular loop" (upcycling). Although conventional high-temperature pyrolysis can achieve relatively high selectivity toward styrene monomers due to the thermodynamic stabilization of polymer radicals by the aromatic pendant groups, the process is inherently bottlenecked by substantial energy penalties, cost-intensive downstream distillation, and extreme sensitivity to additives or impurities in real-world plastic streams. To circumvent these industrial limitations, targeted chemical upcycling strategies focus on the precise transformation of polymer backbones under milder, catalyst-controlled conditions into high-value fine

Downloaded from https://www.cambridge.org/core. 15 Nov 2026 at 12:57:10, subject to the Cambridge Core terms of use.

chemicals, advanced functional materials, or tailored platform molecules. Therefore, the pivotal scientific challenge lies in overcoming the energy barriers of inert chemical bonds under mild conditions to precisely drive this "molecular loop".

To address this formidable challenge, a novel paradigm has been established in recent years through the introduction of "molecular engineering", shifting the degradation of PS from mere destructive cracking to the precise activation of C(sp^3)-C(sp^3) and C-H bonds [31–39]. The research focus is rapidly shifting toward highly selective green catalytic systems (Figure 3). In particular, the rapid development of photocatalytic and electrocatalytic technologies has offered unprecedented opportunities for polymer degradation and controlled electron transfer under ambient conditions (Table 1) [61]. Concurrently, with the continuous enrichment of molecular-level reconstruction methods, the versatile upcycling landscape of aromatic polymers has been profoundly broadened by integrating transformations into porous and optoelectronic materials, as well as biochemical hybrid processes based on a "chemical deconstruction-metabolic funnel" [45,60,62].

Although immense potential is demonstrated by molecular-level conversion strategies, bottlenecks urgently needing to be overcome for industrialization still remain, including catalyst poisoning by impurities in real-world waste plastics, selectivity control in complex blend systems, and the balance between economic feasibility and energy consumption during scale-up. In this review, recent advances in the high-value conversion of waste PS are systematically summarized. The core contents encompass controlled backbone deconstruction mechanisms driven by multiple energy fields (thermal, mechanical, photochemical, and electrical), precise C–H bond functionalization and macroscopic materialization transformations, and emerging biochemical hybrid upcycling processes. Finally, forward-looking perspectives are provided by integrating the synergistic conversion of mixed plastics and comprehensive LCA/TEA—particularly addressing feedstock logistics and pretreatment costs—aiming to offer a theoretical blueprint for constructing a green plastics circular system.

2. Non-Oxidative Deconstruction: Hydrocarbon Products from Backbone Cleavage

The non-oxidative deconstruction of PS targets the cleavage of the inert C(sp^3)–C(sp^3) backbone to recover pure hydrocarbons and platform feedstocks. Lacking the thermodynamic driving force of oxygen insertion, precise chain scission requires specialized catalytic environments and alternative energy inputs. Specifically, C–C cleavage and fragment stabilization are facilitated by reductive hydrogenolysis (Figure 4). Meanwhile, requisite activation energy is supplied by mechanochemical and photothermal modes, and targeted backbone deconstruction is directed by acid-promoted carbocation pathways. By strictly focusing on hydrocarbon and monomer-level recovery without oxygenative functionalization, the highly selective conversion of PS into well-defined aromatic hydrocarbons and liquid fuels has been successfully realized.

2.1 Reductive Hydrogenolysis to Hydrocarbon Fuels and Aromatics

Reductive catalytic strategies provide an effective approach for converting PS into value-added hydrocarbons via sequential hydrogenation and C–C bond cleavage. Within this context, Ni-based non-noble metal catalysts have emerged as promising systems. In 2024, Vlachos' group reported the solvent-free hydrogenolysis of PS to produce lubricant base oils over Ni/SiO_2 catalysts [40]. High-molecular-weight PS (~97 kDa) was converted into group IV base oils with yields up to 70%, exhibiting high viscosity indices (~130) and robust thermo-oxidative stability. Mechanistically, the hydrogenation of aromatic rings precedes C–C backbone cleavage, with structural sensitivity observed at the Ni sites (Figure 5a). Furthermore, catalyst recycling enhanced hydrogenation activity due to the enrichment of Ni(111) facets, although susceptibility to deactivation by additives (e.g., $CaCO_3$) in real wastes remains a challenge. Beyond direct hydrogenolysis, cascade strategies have been explored to transform PS into energy carriers. In 2025, An's group developed a tandem route encompassing pyrolysis, hydrogenation, and dehydrogenation to produce liquid

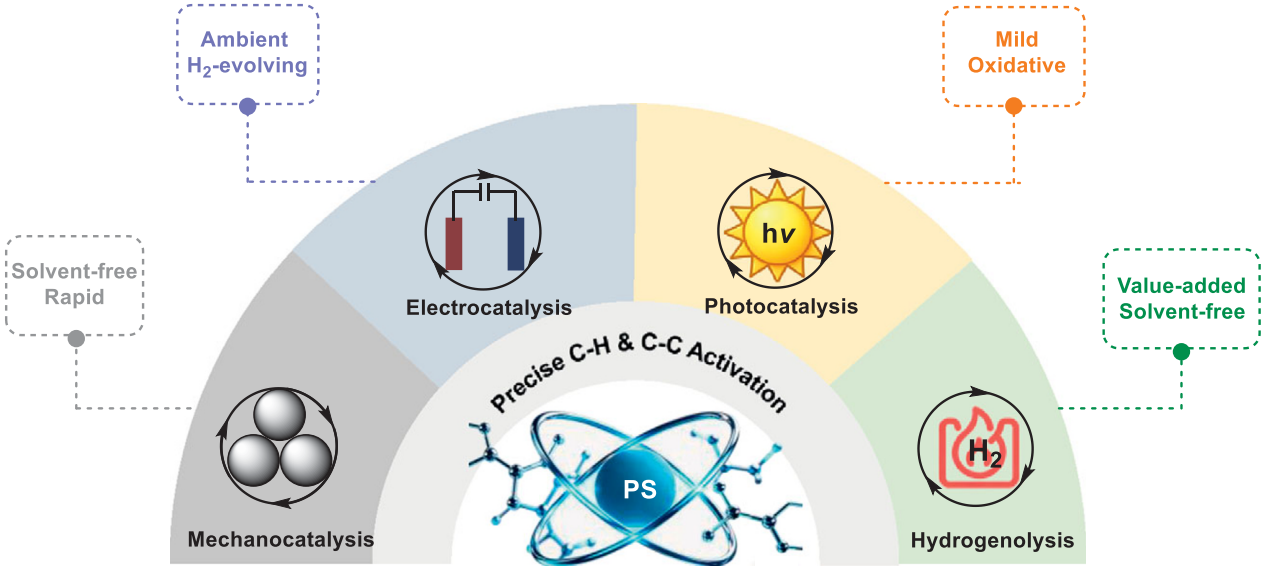


Figure 3. Precise C–H and C–C bond activation strategies based on the core PS catalysis technology.

Downloaded from https://www.cambridge.org/core. 15 Nov 2026 at 12:57:10, subject to the Cambridge Core terms of use.

Table 1. Comprehensive comparison of representative versatile upcycling strategies

Strategy/pathway	Catalyst/system	Energy input and conditions	Key mechanism	Scale & sustainability (LCA/TEA)	Product yield/ selectivity	Energy consumption assessment	Ref
Reductive/ hydrogenolysis	Ni/SiO_2	H_2, solvent-free	Aromatic hydrogenation precedes C–C cleavage via Ni(111) facets	Catalyst recycling enhanced activity	70% yield of lubricant base oils	High: elevated temperature	[40]
Reductive (tandem)	$RuSA/Co_3O_4$	Hydropyrolysis + vapor-phase hydrogenolysis	Isolated Ru sites promote C-C cleavage and suppress over-hydrogenolysis	Excellent stability over 100 h	83.5 wt% yield of toluene, >99% selectivity	High: Two-stage: 475° C + 275°C	[41]
Mechanochemical	$AlCl_3$	Ball milling (30 Hz, 15 min), ambient conditions	Lewis acid-promoted aromatic protonation and carbocation cleavage	Solvent-free, potential closed-loop route	89% degradation extent	Low: Ball milling at room temperature	[42]
Photothermal	Carbon black	White-light/ focused solar irradiation	Localized heating inducing random chain scission and unzipping	Additive-free for black wastes	60% styrene yield; 53%	Low-medium: Solar or white-light driven	[43]
Acid-promoted	Triflic acid	20°C, mild conditions	Carbocation-mediated pathways, challenging traditional β-scission	Selectivity depends on acid concentration	Product distribution depends on acid concentration	Low: 20°C, ambient conditions	[44]
Photocatalytic (LMCT)	$FeCl_3$ or $FeBr_3$	Visible-light (390 or 456 nm), O_2 atm	Halogen radical triggered HAT and β-scission	Mw reduction from >90 to <1 kDa	$FeCl_3$: 67% benzoic acid yield; $FeBr_3$: acetophenone/ benzoic acid ratio up to 2.3:1	Low: Room temp, visible light (390–456 nm)	[40–53]
Thermal oxidation	$NaNO_2$/AcOH + $CoCl_2$	180°C, 2 bar O_2	Dual-site HAT via transient dioxetane	Outperforms vast majority of existing photo/ thermal systems	90% yield of benzoic acid	High: 180°C, 2 bar O_2	[54]
Photoelectrochemical	Fe(TPP)Cl	390 nm + constant-current electrolysis	Synergistic anodic oxidation, cathodic HER (in situ H_2O_2), and Fe-catalyzed HAT	Exceptional tolerance to real wastes	73.7% total yield of benzoyl products	Medium: RT; light + electrolysis	[55]
Divergent (skeletal rearrangement)	$AlCl_3$ then THICA/ NHPI + HNO_3/AcOH	Room temp then 100°C	Macro-to-micro skeletal reorganization to polyindane circumventing spatial constraints	10 g scale demonstration	Phthalic anhydride (yield not explicitly reported)	Medium: RT to 100°C, two-step	[56]
Heteroatom (nitridative)	CuBr + Acetonitrile	200°C, 2 MPa O_2	Trace water-triggered hydroxyl radicals facilitate in situ ammonia release	Homogeneous-to-heterogeneous catalyst recovery	70% combined yield Trifluoromethylation	High: 200°C, 2 MPa O_2	[57]
Precision grafting	$Ru(bpy)_3Cl_2$	Blue-light irradiation, ambient	Photoredox C (sp^2)-H fluoroalkylation	Complete suppression of deleterious chain-scission	degree of functionalization: 19–71 mol%	Low: Room temp, blue light	[58]
Materialization	KOH activation + MgO template	Pyrolysis (700° C) + activation	Pyrolytic carbonization to hierarchical networks	10,000 cycles stability	Hierarchical porous carbon	High:700°C–900°C	[59]

(*Continued*)

Downloaded from https://www.cambridge.org/core. 15 Nov 2026 at 12:57:10, subject to the Cambridge Core terms of use.

Table 1. (*Continued*)

Strategy/pathway	Catalyst/system	Energy input and conditions	Key mechanism	Scale & sustainability (LCA/TEA)	Product yield/ selectivity	Energy consumption assessment	Ref
Biochemical hybrid	Mn/ Br + *Pseudomonas putida* KT2440	Thermocatalytic autoxidation + microbial fermentation	Chemical depolymerization to benzoic acid followed by ortho-cleavage metabolic funnel	LCA/TEA: 61% GHG reduction vs. fossil-derived	94% benzoic acid yield; 61% GHG reduction vs. fossil-based route	Medium: Thermal oxidation + fermentation	[60]

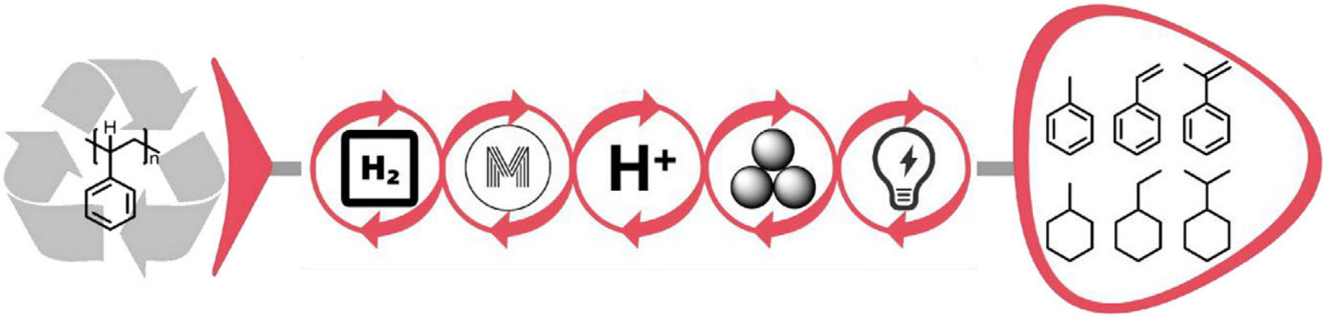


Figure 4. Catalytic reductive upcycling of polystyrene.

organic hydrogen carriers (LOHCs) [46]. Specifically, styrene-rich pyrolytic mixtures were hydrogenated over Ru/C to yield cycloalkanes, which subsequently released hydrogen over Pt/Al_2O_3 catalysts at a rate of 215.5 mmol H_2 $gmetal^{-1}$ min^{-1} at 275°C. Notably, LCA/TEA indicated that this PS-derived LOHC pathway could achieve a negative carbon footprint with competitive hydrogen costs (Figure 5b).

Recently, in 2026, Jiang's group reported a tandem hydropyrolysis-hydrogenolysis strategy for the selective conversion of PS waste into toluene [41]. A dual-stage fixed-bed reactor was utilized to decouple initial pyrolytic deconstruction and catalytic upgrading: PS first undergoes hydropyrolysis at 475°C to form styrene-rich intermediates, which are subsequently converted via vapor-phase hydrogenolysis over a Ru single-atom catalyst supported on Co_3O_4 at 275°C. The catalyst achieved >99% selectivity toward toluene and delivered yields up to 83.5 wt% from post-consumer PS wastes with excellent stability over 100 h. Density Functional Theory（DFT） calculations revealed that isolated Ru sites effectively promote hydrogenation and C–C cleavage while suppressing over-hydrogenolysis. Collectively, these studies from distinct catalytic design perspectives highlight the remarkable versatility of reductive strategies in PS upcycling (Figure 5c). They enable the selective production of bulk commodity aromatics (e.g., toluene) as well as the synthesis of high-performance liquid fuels and hydrogen energy carriers, thereby providing a vital scientific foundation for the resource utilization of plastic waste.

2.2 Mechanochemical Activation and Solid-State Deconstruction

Mechanochemistry offers a highly efficient, solvent-free approach to overcoming the activation energy barriers of inert polymer degradation through mechanical force. In 2025, Wang's group reported a mechanochemical strategy for the rapid degradation of PS to benzene using $AlCl_3$ as a catalyst under ambient conditions [42]. Using ball milling as the energy input, high-molecular-weight PS pellets (165 kDa) were ground with an equal mass of $AlCl_3$ at 30 Hz for 15 min, achieving a degradation extent of 89%. Benzene and low-molecular-weight aliphatic fragments (<250 Da) were obtained as the major products. Mechanistic investigations, including isotope-labeling experiments, indicated that $AlCl_3$ acts as a Lewis acid to promote aromatic protonation, leading to polymer backbone cleavage via carbocation intermediates. Notably, a potential closed-loop recycling route was demonstrated by converting the generated benzene back into styrene via sequential bromination and iron-catalyzed coupling. Alternatively, direct upgrading of PS to benzophenone (40%–50% yield) was achieved through a one-pot cascade Friedel–Crafts acylation performed within the same milling jar (Figure 6). Ultimately, this solvent-free mechanochemical paradigm offers a highly sustainable and rapid pathway for the solid-state upcycling of inert polymers into versatile aromatic building blocks.

2.3 Photothermal-Driven Depolymerization

Distinct from mechanical force, photothermal catalysis leverages localized heating induced by light irradiation to drive endothermic depolymerization processes under macroscopically mild conditions. In 2025, Stache's group reported that carbon black additives, commonly present in commercial plastics, can act as efficient photothermal agents to convert light into localized heat under white-light irradiation [43]. In model systems, PS-carbon black composites afforded styrene yields of up to 60%, whereas neat PS showed no reaction under identical conditions. Mechanistically, the degradation proceeds through random chain scission followed by unzipping depolymerization. This method was successfully applied to various post-consumer black PS wastes (e.g., foam trays and coffee cup lids), producing styrene in yields up to 53% without

Downloaded from https://www.cambridge.org/core. 15 Nov 2026 at 12:57:10, subject to the Cambridge Core terms of use.

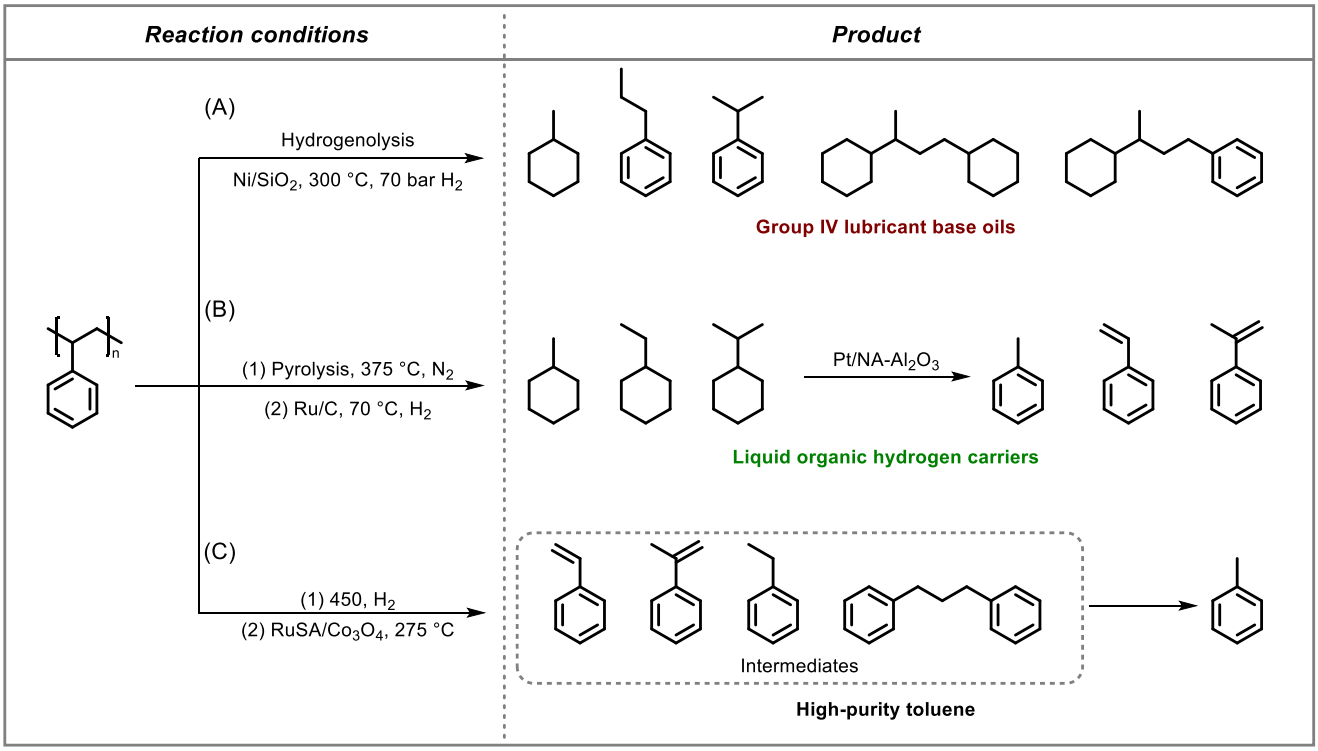


Figure 5. Reductive/hydrogenolysis pathways for PS: (a) direct hydrogenolysis catalyzed by Ni/SiO_2. (b) two-step pyrolysis-hydrogenation-aromatization process. (c) One-pot synthesis of high-purity toluene catalyzed by $RuSA/Co_3O_4$.

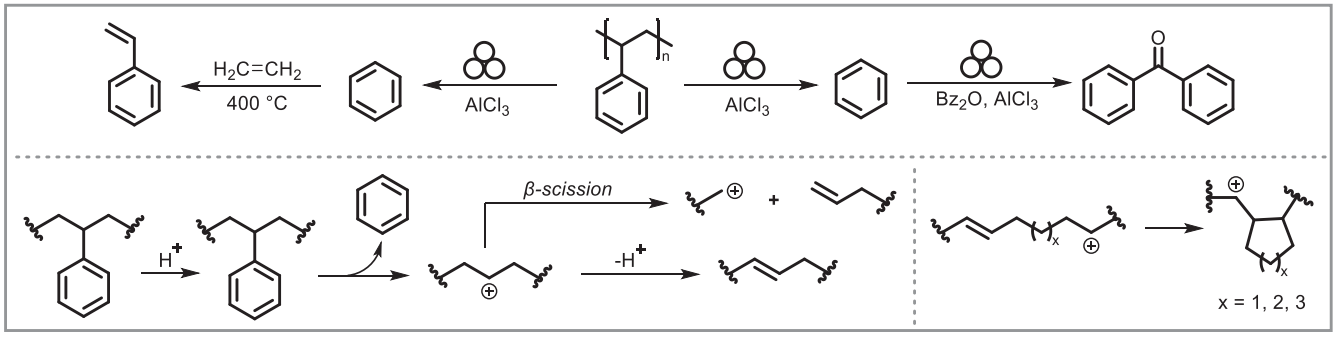


Figure 6. Mechanism for acid-catalyzed PS degradation and upcycling. PS undergoes $AlCl_3$-catalyzed cleavage to benzene, which is then converted to benzophenone via Friedel–Crafts acylation.

the need for additional catalysts. Under focused solar irradiation, an 80% styrene yield was reached within 5 min from black PS foam. Moreover, the addition of only 10 wt% black PS enabled the rapid depolymerization of mixed-color PS wastes, affording styrene yields of 67%–72% under natural sunlight (Figure 7). By ingeniously repurposing intrinsic plastic additives as powerful photothermal susceptors, this solar-driven approach establishes a highly sustainable, self-catalyzed paradigm for closed-loop monomer recovery.

2.4 Acid- and Base-Promoted Deconstruction

Beyond reductive hydrogenolysis and mechanochemical approaches, acid- and base-promoted deconstruction offers complementary pathways for cleaving the inert PS backbone through carbocation-mediated (acid) or carbanion-mediated (base) mechanisms. Depending on the catalyst acidity/basicity and reaction conditions, these strategies enable selective conversion of PS into either styrene monomer or functionalized aromatic building blocks.

Early investigations into ionic-mediated degradation frequently explored single-function solid base catalysts like magnesium oxide (MgO) [47]. As demonstrated in foundational studies, while basic sites successfully enhance the initiation rate via proton abstraction from tertiary carbons, they simultaneously shorten the "zip length" during depropagation due to premature chain termination on the catalyst surface. Similarly, traditional solid acid catalysts effectively provoke carbocation-mediated bond cleavage, yet they traditionally lack high monomer selectivity. In 2023, Lee's group investigated the

Downloaded from https://www.cambridge.org/core. 15 Nov 2026 at 12:57:10, subject to the Cambridge Core terms of use.

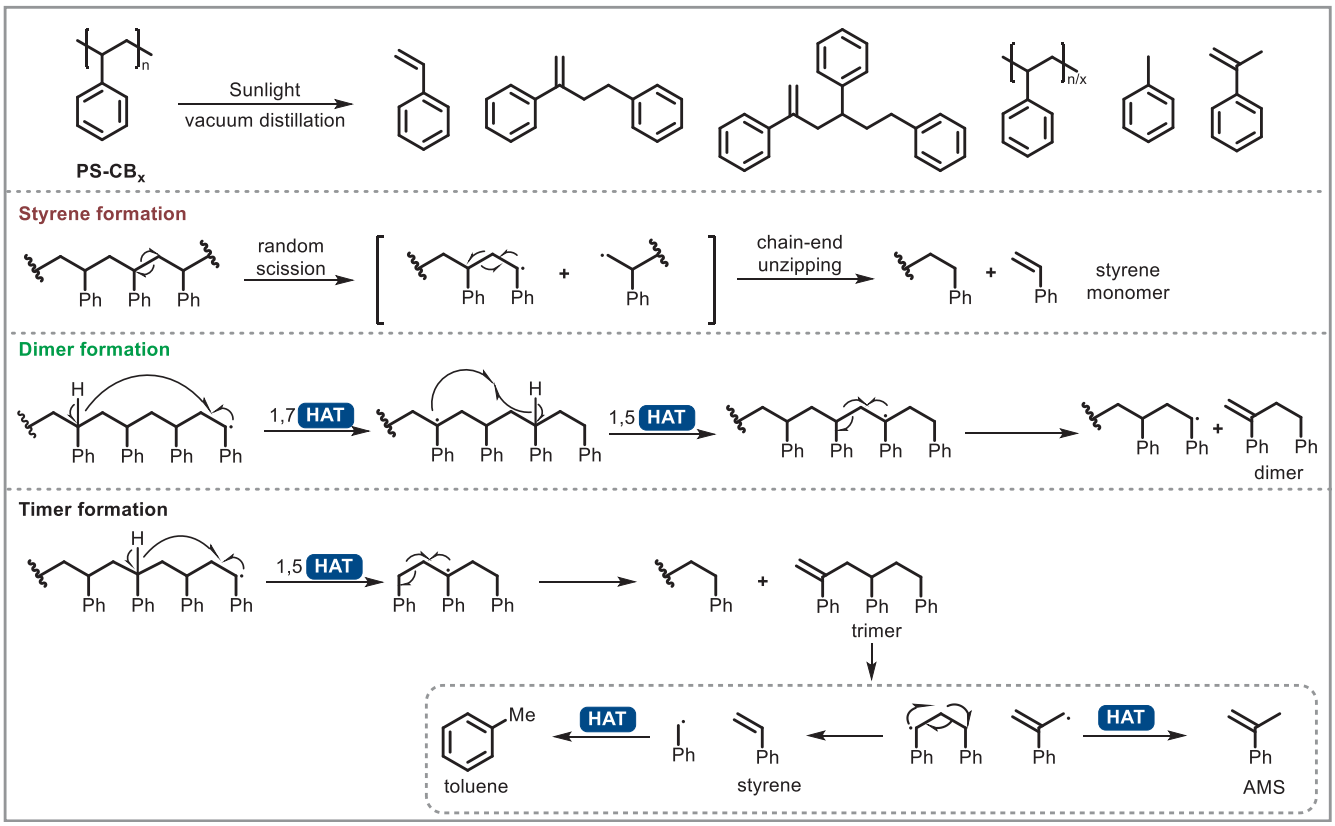


Figure 7. Mechanism of sunlight-driven PS degradation under vacuum distillation. PS decomposes into styrene, oligomers, and aromatics (toluene, AMS) via chain scission, unzipping, and HAT pathways.

mechanism of superacid-assisted degradation of PS using triflic acid under mild conditions [48]. By combining deuterated PS (d8-PS-50) with ^{1}H NMR analysis, proton–deuterium exchange was found to occur at the phenyl ring and β-hydrogens, whereas α-hydrogens remained unreactive, challenging the traditionally proposed β-scission pathway. The degradation at 20°C proceeds through multiple stages depending on acid concentration. At low acid loading, interchain coupling dominates, whereas higher acid concentrations promote intrachain cross-linking and the formation of poly(styrene-co-indan) nanoparticles ($M_w \approx$ 3–10 kDa). Upon prolonged reaction (>48 h), these intermediates further degrade into small aromatic molecules including benzene, alkylbenzenes, indan derivatives, and diphenylmethane, which can subsequently undergo Scholl-type reactions to generate polycyclic aromatic hydrocarbons such as pyrene and phenanthrene. Collectively, this work underscores the unique ability of strong Brønsted acids to direct PS deconstruction through carbocation-mediated pathways, revealing that product distributions are finely dictated by acid strength and concentration. To achieve higher selectivity toward hydrocarbon products, attention shifted toward solid base catalysts. In 2026, Zhang's group developed a highly efficient defective zinc aluminate spinel catalyst [49], ZAS-16(Vo), for solvent-assisted polystyrene deconstruction. By introducing precise oxygen vacancies (Vo) through structural distortion and cation disorder, the catalyst successfully modulated surface electronic structures—weakening Zn–O bonds and concentrating well-matched Lewis acid–base site pairs. Coupled with toluene as a dynamic solvent that promotes polymer chain disentanglement and mitigates mass-transfer "cage effects," this integrated Lewis acid–base synergy achieved an exceptional 98.82 wt% conversion and a 76.21 wt% styrene yield at a mild temperature of 350°C. Mechanistically, the adjacent Lewis acid sites initiate the process via hydride abstraction to form benzylic carbocations followed by β-scission, while the basic sites stabilize key carbanion intermediates through aromatic ring delocalization to steer selective cracking.

2.5 Summary

Overall, non-oxidative catalytic deconstruction strategies establish a robust framework for activating the inert C(sp^3)–C(sp^3) backbone of PS, enabling its precise deconstruction into value-added hydrocarbons and aromatic building blocks. Despite these conceptual and technological breakthroughs, formidable challenges remain in bridging the gap toward practical applications, particularly regarding the enhancement of catalytic selectivity, the optimization of energy efficiency, and the improvement of intrinsic tolerance toward the complex heterogeneities of real-world plastic wastes. From a sustainability perspective, non-oxidative strategies show considerable divergence. Reductive hydrogenolysis delivers high-value hydrocarbons but incurs energy penalties from H_2 atmosphere and elevated temperatures. Mechanochemical and photothermal approaches operate under milder conditions with minimal solvent use, yet the former relies on stoichiometric $AlCl_3$ and the latter is limited to dark-colored waste streams. Acid-promoted deconstruction avoids thermal costs but introduces corrosive reagent disposal burdens. These trade-offs suggest that strategy selection must be guided by feedstock characteristics and acceptable environmental burden.

Downloaded from https://www.cambridge.org/core. 15 Nov 2026 at 12:57:10, subject to the Cambridge Core terms of use.

3. Catalytic Oxidative Upcycling of PS

Distinct from non-oxidative pathways yielding pure hydrocarbons, the catalytic oxidative upcycling of PS targets the selective activation and oxygenation of benzylic C–H bonds [50]. This approach transforms the inert polymer backbone into value-added oxygenated aromatics (e.g., benzoic acid, benzaldehyde, acetophenone), which serve as critical intermediates for fine chemical industries. Under macroscopically mild conditions, these transformations are successfully driven by diverse energy inputs, encompassing photocatalytic, thermal/acid-promoted, and emerging photoelectrochemical systems. Through rational catalyst design, the underlying radical or ionic mechanisms are effectively regulated, enabling precise control over product selectivity (Figure 8).

3.1 Homogeneous Photocatalytic Oxidation Systems

Despite their diverse catalyst structures and activation modes, all homogeneous photocatalytic oxidation systems share a common mechanistic blueprint: benzylic C–H abstraction → O_2 trapping → peroxyl radical formation → β-scission → oxidative cascade to oxygenated aromatics. The core distinction among these systems lies primarily in the initiation step, which dictates the overall efficiency and selectivity. The following subsections focus on these distinctive initiation pathways, while the common mechanistic framework is summarized in Table 2. Homogeneous photocatalytic systems represent one of the most widely explored strategies for the oxidative upcycling of PS. Depending on the primary active species and the specific bond-activation mechanisms involved, these homogeneous systems can generally be categorized into ligand-to-metal charge transfer pathways, direct hydrogen atom transfer (HAT) pathways, reactive oxygen species (ROS)-mediated pathways, and metal-centered redox/single-electron transfer (SET) pathways.

3.1.1 Ligand-to-Metal Charge Transfer (LMCT) Pathways

LMCT has emerged as a powerful photochemical mechanism for generating highly reactive halogen radicals to initiate polymer degradation. In a series of studies starting in 2021, Zeng's group and Stache's group independently developed inexpensive $FeCl_3$-catalyzed photocatalytic systems for PS oxidation [44,51]. Under visible-light irradiation (390 nm) in O_2, LMCT excitation of $FeCl_3$ generates •Cl radicals that initiate the unified HAT/O_2/β-scission cascade (see Section 3.1), yielding benzoic acid (up to 67%) and benzaldehyde (Figure 9a). This strategy demonstrated excellent compatibility with commercial PS foams and led to dramatic molecular weight reduction (e.g., from >90 to <1 kDa). To further control product selectivity, the Stache's group systematically compared $FeCl_3$ and $FeBr_3$ as radical precursors [52,53]. Mechanistic studies revealed that highly reactive •Cl abstracts both secondary and tertiary C–H bonds indiscriminately, predominantly yielding benzoic acid. Conversely, the less reactive bromine radical (•Br) selectively abstracts tertiary C–H bonds. Furthermore, the intermediate primary alkyl radicals can undergo HAT with HBr (forming methyl chain ends), shifting the product distribution toward acetophenone. By adjusting the halogen precursor and introducing LiBr, an acetophenone-to-benzoic acid ratio of up to 2.3:1 was achieved, demonstrating that tuning LMCT-derived radical reactivity is a powerful tool for regulating product divergence (Figure 9b). This contrasting behavior—indiscriminate HAT by chlorine radicals versus selective tertiary C–H bond activation by bromine radicals—demonstrates that tuning the reactivity of LMCT-derived radicals enables controlled product divergence between benzoic acid and acetophenone.

3.1.2 Direct HAT Pathways

Organic HAT photocatalysts offer an attractive, metal-free alternative for PS oxidative deconstruction under mild conditions. Organic HAT photocatalysts abstract benzylic hydrogens upon photoexcitation, initiating the unified HAT/O_2/β-scission cascade.

In 2022, Reisner's group reported the photocatalytic oxidative degradation of PS using fluorenone as a HAT photocatalyst. Under blue light irradiation (50°C) and ambient O_2, excited-state fluorenone abstracts benzylic hydrogen to form a ketyl radical [63]. The concurrently generated PS benzylic radical undergoes rapid oxygenation and β-scission, efficiently converting high-molecular-weight PS (260 kDa) into benzoic acid (~40%) and other monocyclic aromatics. Gel permeation chromatography (GPC) analysis confirmed a rapid molecular weight reduction to 3.2 kDa within 4 h, leading to complete deconstruction after 16 h (Figure 10a). Building upon this metal-free paradigm, the Kokotos's group developed an aerobic upcycling strategy in 2023 utilizing anthraquinone (AQ) as a photosensitizer [64]. Under 390 nm irradiation, the highly electrophilic triplet excited state of AQ initiates the degradation via a similar semiquinone-mediated HAT process. Utilizing air as the sole oxidant, this protocol eliminated the need for strong acids or halogens and exhibited broad applicability across commercial PS

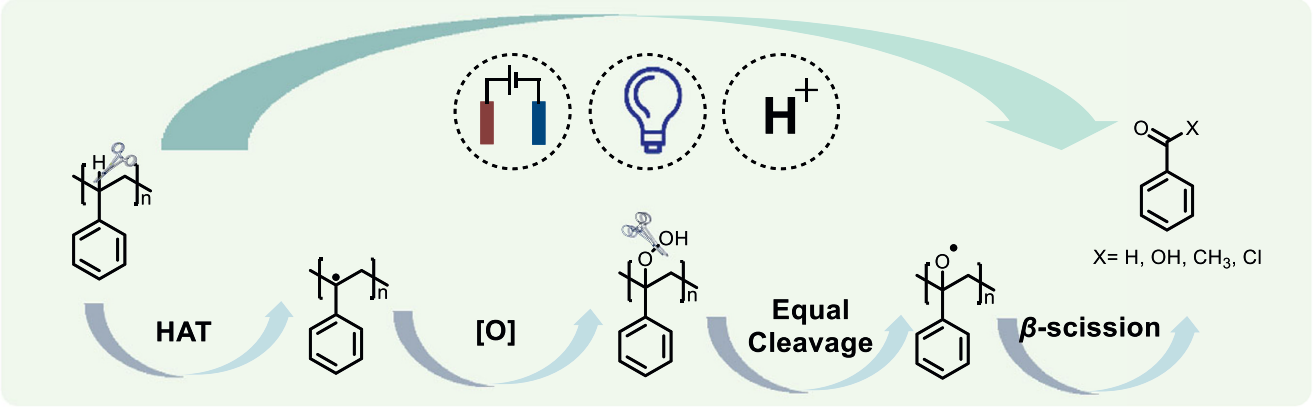


Figure 8. Catalytic oxidative upcycling of PS.

Downloaded from https://www.cambridge.org/core. 15 Nov 2026 at 12:57:10, subject to the Cambridge Core terms of use.

Table 2. Mechanistic framework for polystyrene oxidative upcycling: contrasting initiation pathways, driving forces, and product fates.

Mechanistic dimension	Pathway/control type A	Pathway/control type B	Key differences & impact on PS upcycling
Initiation mechanism	**Direct HAT pathway:** Catalyst directly abstracts a benzylic hydrogen atom from the polymer backbone.	**ROS-mediated pathway:** Catalyst first activates ambient O_2 into reactive oxygen species	**Selectivity vs. kinetics:** Direct HAT strictly depends on BDE matching, offering high site-selectivity. ROS pathways exhibit faster overall kinetics but often suffer from indiscriminate attacks lowering selectivity.
Reaction driving forces	**Kinetic control:** Determined by the activation energy barriers of the rate-limiting steps	**Thermodynamic control:** Determined by the overall free energy change ($\triangle G$) of the reaction.	**Barrier vs. sink:** Breaking the inert benzylic Csp^3-H bond and the β-scission of C–C bonds impose severe kinetic barriers. Conversely, the deep exergonic well of forming stable oxygenates (e.g., benzoic acid) acts as the thermodynamic driving force.
Product fate	**Selective oxidation:** Targeted cleavage yielding specific value-added aromatic oxygenates.	**Over-oxidation (mineralization):** Uncontrolled, successive oxidation leading to complete combustion into CO_2 and H_2O	**The "Kinetic Pause":** To prevent mineralization, successful catalysts must ensure that the generated small molecules possess a higher kinetic barrier toward further oxidation than the parent polymer, allowing for product isolation.

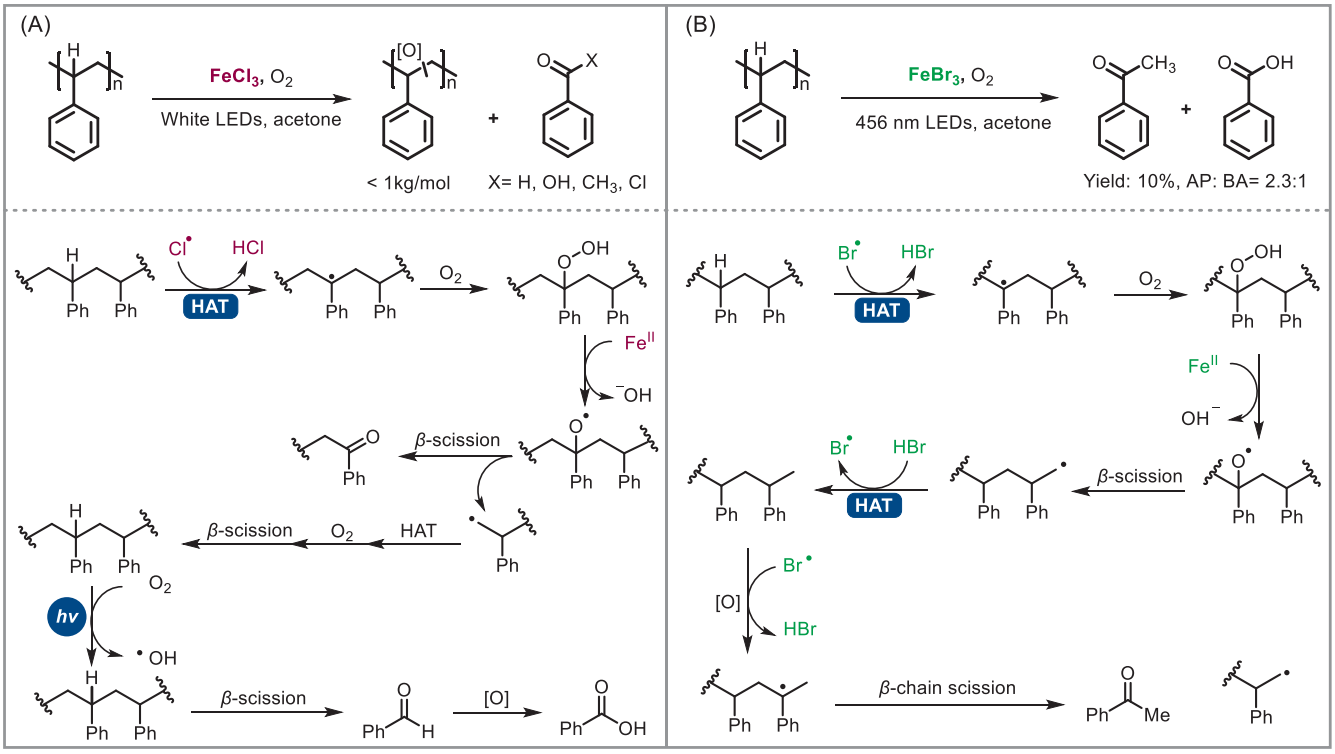


Figure 9. Mechanisms of Fe(III)-catalyzed PS photodegradation under LEDs. (a) $FeCl_3/O_2$ under white light forms oxidized oligomers and aromatic carbonyls. (b) $FeBr_3/O_2$ under 456 nm light yields acetophenone and benzoic acid (2.3:1 ratio). Both proceed via HAT, oxygen addition, and β-scission.

wastes, affording benzoic acid yields ranging from 25% to 58%. More recently, in 2025, Xiao's group achieved highly efficient plastic upcycling using a phenothiazine-based photocatalyst (PTH-3CN) [65]. Operating via a consecutive photoinduced electron transfer (conPET) mechanism—where the catalyst absorbs two successive photons to access an exceptionally potent oxidative excited state—this system converted PS to benzoic acid (50%) and formic acid under 405 nm irradiation with an extremely low catalyst loading (500 ppm). Notably, this method demonstrated exceptional universality across diverse plastics (e.g., SAN, ABS, PE, PVC). While these organic HAT systems provide a versatile, metal-free platform for PS upcycling (Figure 10b).

3.1.3 Reactive Oxygen Species (ROS)-Mediated Pathways

In ROS-mediated pathways, molecular oxygen is preferentially activated by the photocatalyst, rather than the polymer substrate being directly engaged. The photogenerated ROS—such as singlet oxygen or superoxide radical anions—serve as the primary active species to abstract benzylic hydrogen atoms, thereby initiating the radical cascade that leads to oxidative chain scission. In 2022, Das's group reported a metal-free photocatalytic strategy for converting PS into aromatic building blocks [66]. By utilizing *N*-bromosuccinimide (NBS) as a bromine source and sodium trifluoromethanesulfinate as an additive, PS was efficiently oxidized to benzoic acid (up to 73% yield) under 390 nm irradiation in an O_2 atmosphere (Figure 11). This mild protocol was successfully

Downloaded from https://www.cambridge.org/core. 15 Nov 2026 at 12:57:10, subject to the Cambridge Core terms of use.

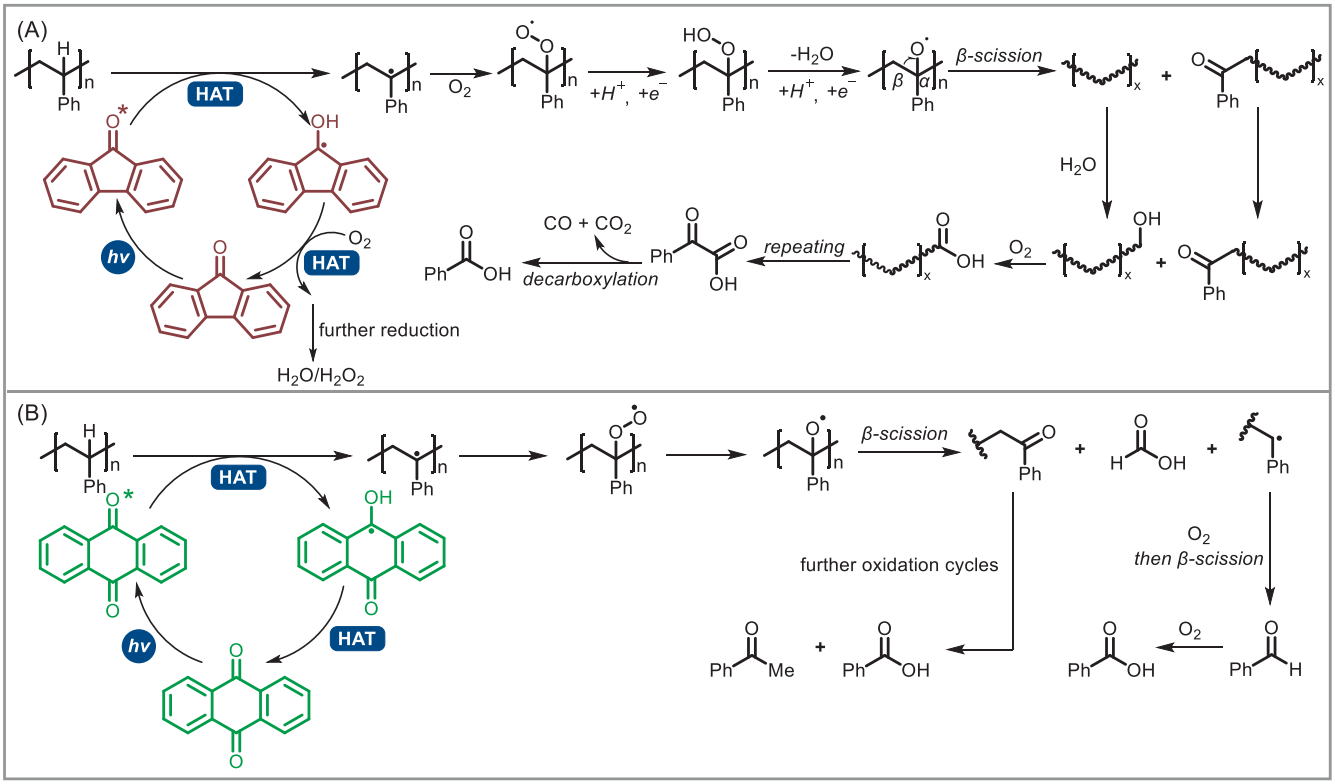


Figure 10. Mechanisms of photocatalytic PS degradation mediated by different ketone catalysts. (a) Fluorenone-catalyzed pathway: proceeds via HAT, oxygen addition, and *β*-scission to form carboxylic acids, which undergo further decarboxylation. (b) Anthraquinone-catalyzed pathway: involves direct HAT from sp^3 C–H bonds, followed by oxidation and *β*-scission to yield aromatic carbonyl products.

applied to various real-world PS wastes (e.g., foam plastics, yogurt containers), affording benzoic acid yields of 51%–68%. Mechanistically, it was suggested that photolysis generates bromine radicals and reactive sulfur species, which cooperatively facilitate the initial HAT process. Crucially, the involvement of superoxide radicals ($\bullet O_2^-$) was confirmed by electron paramagnetic resonance (EPR) spectroscopy, and the origin of the incorporated oxygen atoms from molecular O_2 was unambiguously verified via isotope-labeling studies. More recently, in 2025, Taton's group re-examined the underlying photophysical mechanisms of acridinium-catalyzed PS upcycling [17]. Using 9-mesityl-10-methylacridinium perchlorate under 456 nm irradiation, PS was degraded into benzoic acid (~40%) and formic acid. Through time-resolved emission and transient absorption spectroscopy, it was revealed that the excited-state MA is preferentially quenched by molecular oxygen rather than the PS substrate. Computational analyses further indicated that approximately 77% of absorbed photons are channeled into ROS generation (via energy or SET), whereas merely ~1% are consumed by direct polymer interaction. While these ROS-driven paradigms provide a highly sustainable, metal-free oxidation route, precise control over specific ROS generation efficiency remains a critical hurdle to mitigate over-oxidation and enhance product selectivity.

3.1.4 Metal-Centered Redox and SET Pathways

Transition-metal complexes provide versatile platforms for mediating benzylic C-H activation by elegantly coupling photochemistry with metal-centered SET and redox cycling. Upon photoexcitation, highly oxidizing metal centers can directly abstract hydrogen atoms or initiate SET, driving subsequent oxidative C–C bond cleavage under macroscopically mild conditions.

In 2023, Soo's group reported a visible-light-driven oxidative degradation system utilizing commercially available vanadyl acetylacetonate ($VO(acac)_2$) [67]. Under white LED irradiation and an O_2 atmosphere in dichloromethane, PS was smoothly converted into value-added platform chemicals (e.g., benzoic acid and formic acid). Mechanistic investigations—integrating kinetic analysis, EPR, XPS, and DFT calculations–revealed a tandem catalytic cycle. Specifically, the photo-induced oxidation of V(IV) generates a reactive V(V) species that facilitates rate-determining benzylic hydrogen abstraction, followed by rapid oxygen capture and C–C scission. Impressively, this protocol was successfully scaled up in a continuous-flow photoreactor and exhibited robust tolerance toward contaminated foams and multilayer packaging (e.g., PS-EVOH-PS).

In the same year, Jiang's group developed an unconventional uranyl (UO_2^{2+}) photocatalytic system for the selective degradation of styrenic plastics [45]. Using uranyl nitrate under blue-light irradiation (460 nm), PS and its copolymers were efficiently degraded to benzoic acid. Mechanistic studies suggested that the highly oxidizing excited uranyl species ($^*UO_2^{2+}$) activates benzylic C–H bonds through a synergistic combination of direct HAT and SET pathways. The applicability of this method was further demonstrated across various styrenic blends (EPS, HIPS, SAN, ABS) and could even be extended to heterochain plastics (PET, PC). While these metal-centered redox pathways showcase exceptional mechanistic versatility, inherent environmental concerns regarding heavy metal toxicity underscore the pressing need

Downloaded from https://www.cambridge.org/core. 15 Nov 2026 at 12:57:10, subject to the Cambridge Core terms of use.

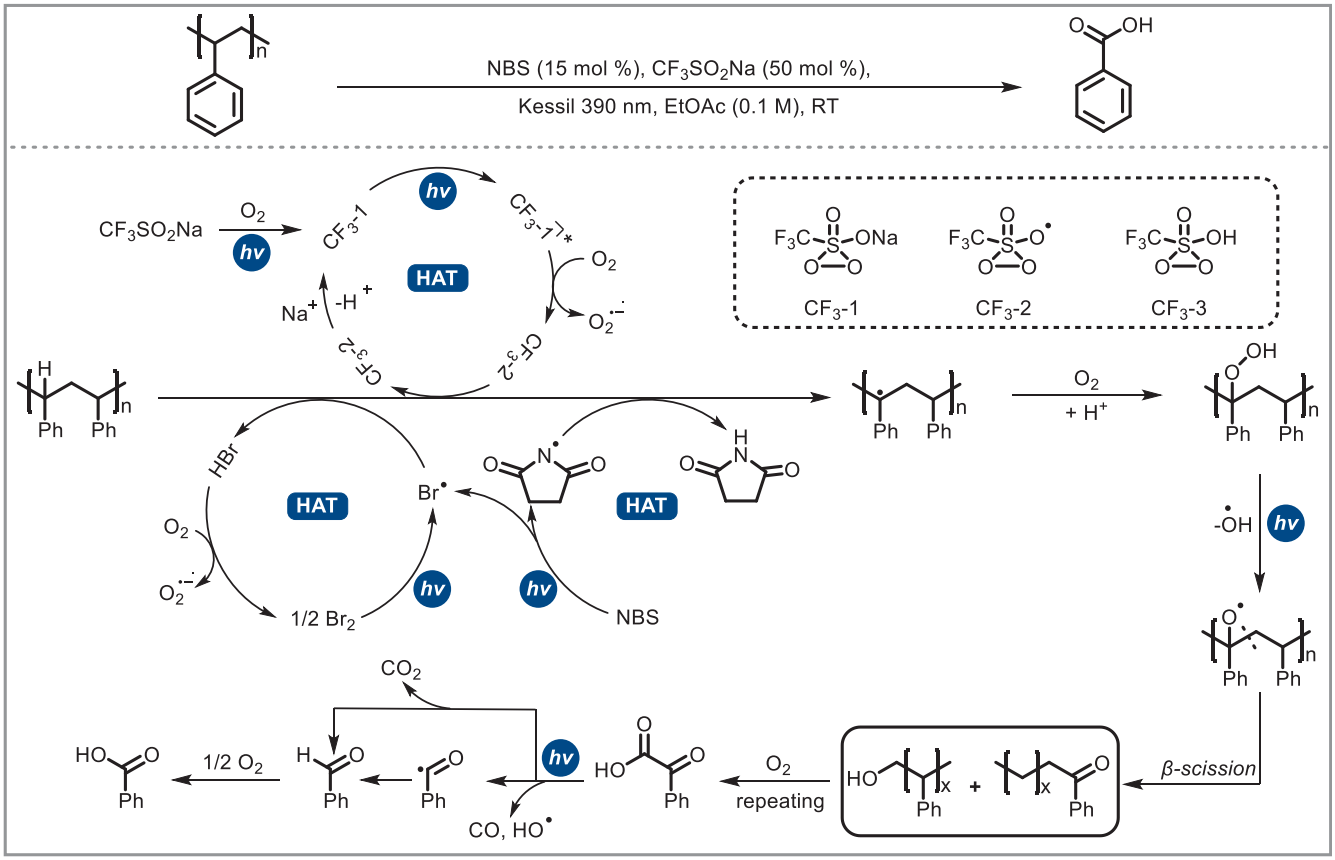


Figure 11. Proposed mechanism for the photochemical degradation of PS to benzoic acid using NBS/CF_3SO_2Na under 390 nm light. The process involves dual HAT cycles (NBS and CF_3SO_2Na-derived radicals), oxygen addition, β-scission, and repeated oxidation steps to yield benzoic acid.

for more benign and sustainable transition-metal alternatives (Figure 12).

3.1.5 Summary

In summary, homogeneous photocatalytic systems provide versatile and highly tunable platforms for the oxidative upcycling of PS under macroscopically mild conditions. By elegantly leveraging distinct mechanistic pathways—ranging from LMCT-induced halogen radicals and direct organic HAT to ROS-mediated oxidations and metal-centered SET processes—researchers have achieved precise activation of benzylic C–H bonds. These mechanistic advancements have enabled the selective deconstruction of the inert polymer backbone into specific oxygenated aromatics, such as benzoic acid and acetophenone. However, despite their exceptional catalytic efficiency and mechanistic clarity, homogeneous systems face inherent practical challenges, particularly regarding catalyst recovery, strong solvent dependence, and limitations in large-scale continuous processing. Addressing these sustainability and scalability bottlenecks remains a critical frontier, logically driving the ongoing development of robust heterogeneous catalytic paradigms.

3.2 Heterogeneous Semiconductor Photocatalysis

Heterogeneous semiconductor photocatalysts offer a robust and sustainable platform for PS upcycling, characterized by their structural stability, recyclability, and ease of phase separation [68,69]. Unlike molecular catalysts, semiconductors utilize photo-induced charge carriers to activate molecular oxygen at the solid–liquid interface. Depending on the material composition and surface modification, these heterogeneous systems can be primarily categorized into carbon-based semiconductors and metal-oxide systems.

3.2.1 Metal-Free Carbon-Based Semiconductors

Graphitic carbon nitride (g-C_3N_4) has emerged as a cornerstone of metal-free PS upcycling due to its visible-light responsiveness and favorable band alignment for O_2 activation. In 2022, Ma's group reported a thermal condensation-derived g-C_3N_4 system for the oxidative degradation of PS (Figure 13). Under visible light (150°C, 10 bar O_2), PS was successfully converted into aromatic oxygenates (benzoic acid, acetophenone, and benzaldehyde) [70]. Detailed investigations revealed that photogenerated electrons on the g-C_3N_4 surface drive the formation of $\bullet O_2^-$, which serve as the primary species for benzylic C–H abstraction. The system achieved a benzoic acid selectivity of >80%, demonstrating that pure organic semiconductors can rival metal-based systems in polymer deconstruction.

3.2.2 Metal Oxide-Based Semiconductors

Metal oxides, particularly TiO_2, remain the most extensively studied photocatalysts owing to their exceptional photostability and potent oxidizing power. To overcome the limited visible-light absorption of neat TiO_2, surface functionalization strategies have been widely adopted. In 2023, Li′s group developed an organically

Downloaded from https://www.cambridge.org/core. 15 Nov 2026 at 12:57:10, subject to the Cambridge Core terms of use.

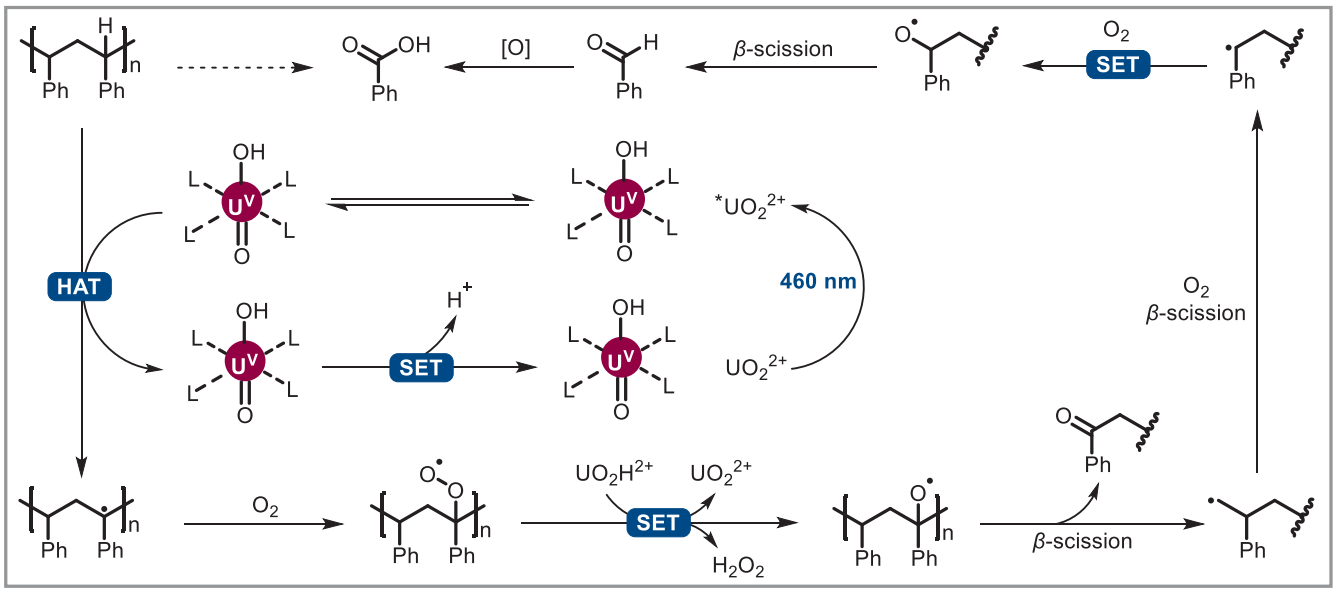


Figure 12. Mechanism of uranyl-catalyzed photodegradation of PS under 460 nm irradiation. The process involves HAT and SET steps, followed by oxygen addition and *β*-scission to yield benzoic acid.

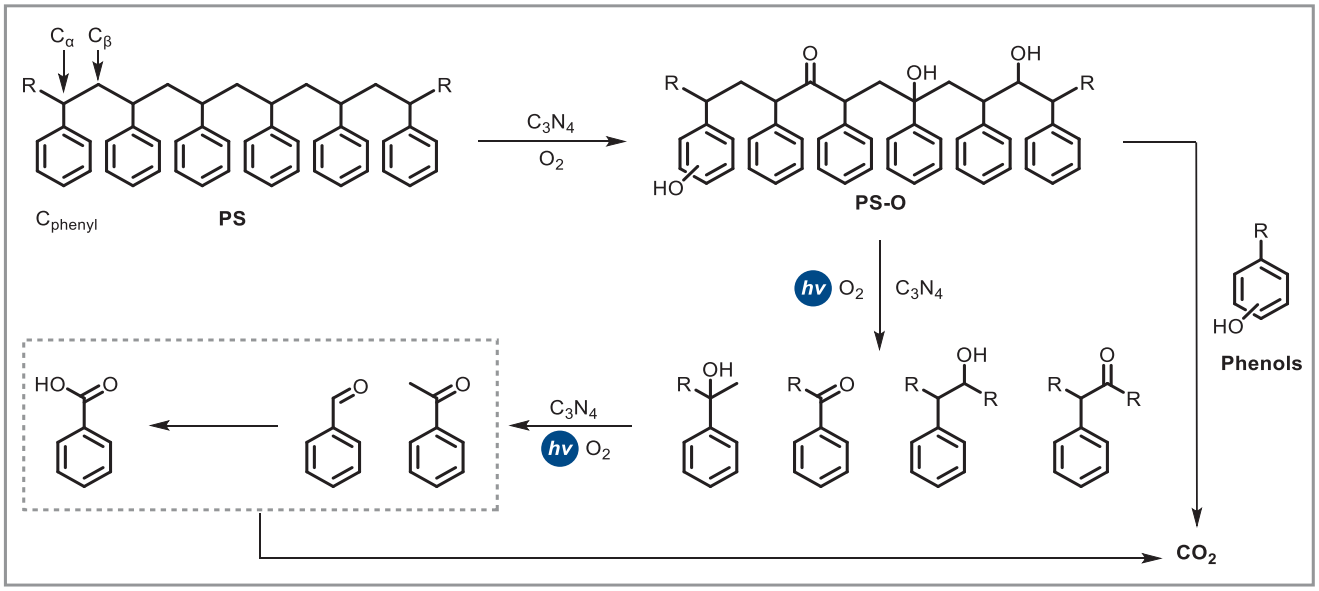


Figure 13. Schematic of the stepwise photodegradation of PS mediated by g-C_3N_4 under oxygen. The process proceeds via initial oxidation to oxygenated PS (PS-O), followed by chain cleavage to aromatic intermediates, and final mineralization to benzoic acid, phenols, and CO_2.

modified TiO_2 system using potassium stearate and nitrogen-containing silanes [71]. This surface engineering not only enhanced the hydrophobicity of the catalyst for better polymer contact but also facilitated proton-coupled electron transfer (PCET). Under 370 nm irradiation, PS was converted to benzoic acid with yields up to 43.5 mol% under ambient conditions. The strategy's versatility was further validated using real-world wastes like yogurt cups and pipette tips, highlighting its practical potential.

3.2.3 Porous Organic Polymer-Based Photocatalysts

To further circumvent the harsh operating conditions (e.g., elevated temperatures and high pressures) often associated with early solid-state photocatalysts, porous organic polymers like covalent triazine frameworks (CTFs) have recently gained traction. In 2026, Mohamed's group reported a novel iron-doped covalent triazine framework ([$FeCl_4$]@CTF) for the highly efficient heterogeneous photocatalytic deconstruction of PS under strictly ambient conditions [72]. Synthesized via scalable, solvent-free mechanochemistry, this donor-acceptor polymer matrix features $FeCl_4^-$ anions cross-linking 2D sheets via Fe–S coordination bonds, requiring an ultra-low iron loading of less than 3 wt%. Under visible light irradiation and 1 bar O_2 at room temperature, this composite achieved complete degradation of both commercial and post-consumer PS wastes, yielding approximately 70% valuable aromatic oxygenates

Downloaded from https://www.cambridge.org/core. 15 Nov 2026 at 12:57:10, subject to the Cambridge Core terms of use.

(predominantly benzoic acid). Mechanistically, the heteroatom-rich porous framework not only facilitates the adsorption of oxygen and polymer fragments but also drives a precise LMCT process. This synergistic electronic interaction stabilizes photogenerated charge carriers, facilitating a SET cascade that sequentially generates potent $\bullet O_2^-$ and $^1O_2$ species for targeted benzylic C–H activation. Crucially, the utilization of earth-abundant metals combined with a scalable solid-state synthetic route provides a highly sustainable, recoverable blueprint for industrial-scale plastic upcycling.

3.2.4 Summary

In summary, heterogeneous semiconductor photocatalysis provides a robust and scalable approach for the oxidative upcycling of PS. While metal-free systems like g-C_3N_4 offer sustainable alternatives and modified TiO_2-based materials show excellent stability under ambient conditions, challenges regarding reaction kinetics and visible-light utilization efficiency persist. Addressing the intrinsic activity-stability paradox through rational structural modifications remains a critical frontier for translating these heterogeneous paradigms into practical, large-scale plastic waste management solutions.

3.3 Acid-Promoted Photosensitizer-Free Pathways

While the aforementioned photochemical strategies strictly rely on exogenous metal complexes or organic dyes to harvest light, an emerging frontier explores photosensitizer-free paradigms. In a conceptual breakthrough in 2022, Xiao's group developed an acid-catalyzed photochemical system that drives PS oxidation without the need for any external photocatalysts [61]. Utilizing strong Brønsted acids (e.g., trifluoromethanesulfonic acid, sulfuric acid, or p-toluenesulfonic acid) under 405 nm irradiation and 1 bar O_2, commercial PS was selectively converted into benzoic acid (36%–51% isolated yield) and formic acid (57%–72%). Mechanistic investigations revealed a unique autophotocatalytic pathway: the protonation of the PS backbone forms a distinct [PS···H^+] ground-state complex. This transient complex directly absorbs light to generate $^1O_2$ in situ, which subsequently abstracts tertiary benzylic hydrogen atoms to initiate the oxidative cascade. The viability of this methodology was further demonstrated through gram-scale deconstruction in a continuous-flow reactor using various real-world PS wastes. Although this pioneering work elegantly proves the feasibility of photosensitizer-free upcycling, the reliance on highly corrosive strong acids and the currently moderate product selectivity highlight the necessity for future optimizations in this nascent direction.

3.4 Thermally Driven Catalytic Oxidation Pathways

Beyond photochemical interventions, thermally driven catalytic oxidation represents a robust and scalable paradigm for PS upcycling. By leveraging elevated thermal energy to overcome the intrinsically high activation barriers of inert C–H bonds, these systems typically employ transition-metal-mediated autoxidation or in situ generated radical mediators to facilitate exhaustive oxygenative cleavage.

In 2023, Lim's group reported the first metal-free thermal organocatalytic method for PS oxidation to benzoic acid (BA) and 4-nitrobenzoic acid (4-NBA) using N-hydroxyl catalysts (THICA or NHPI) with HNO_3 in acetic acid at 120°C under air [73]. The reaction proceeds via N-oxyl radical-mediated HAT from the PS backbone, followed by O_2 incorporation and β-scission, yielding BA (up to 32%) and 4-NBA (up to 10%). The exclusive para-nitration arises from steric hindrance during aromatic nitration prior to chain cleavage. This metal-free protocol tolerates colored additives and extends to PS derivatives (e.g., poly(4-methylstyrene) to terephthalic acid; PSS to 4-sulfobenzoic acid), establishing organocatalysis as a viable, additive-tolerant platform for PS upcycling. In 2024, Jiao's group reported a Co/Mn/Br ternary catalytic system—conceptually reminiscent of industrial hydrocarbon oxidation—capable of universally converting mixed polyolefin wastes into valuable carboxylic acids [74]. Utilizing $CoCl_2{\cdot}6H_2O$ and $MnSO_4{\cdot}H_2O$ with HBr as a promoter in n-butyl acetate, PS was oxidatively transformed into benzoic acid (up to 75% yield) at 120° C under ambient O_2 pressure. Remarkably, this robust protocol exhibited broad universality across diverse polyolefins, converting polyethylene (LDPE/HDPE) into C_4–C_7 dicarboxylic acids and polypropylene into acetic and formic acids. The practicality of this system was further underscored by its excellent catalyst recyclability and successful application to complex, mixed-plastic waste streams. More recently, in 2025, Mei's group developed an exceptionally selective thermal oxidation strategy, utilizing nitrogen dioxide (NO_2) as a unique HAT catalyst alongside a $CoCl_2$ cocatalyst [54]. In this system, NO_2—generated in situ from sodium nitrite and acetic acid—served as the primary HAT reagent. Under 180° C and 2 bar O_2, PS was completely degraded within 12 h, affording benzoic acid in an unprecedented yield of up to 90%, thereby outperforming the vast majority of existing photocatalytic and thermal systems. Mechanistic elucidations revealed a distinct dual-site activation pathway: NO_2 simultaneously activates both the C_α–H and C_β–H bonds, promoting the formation of a transient dioxetane intermediate. The subsequent O–O and C–C bond scissions selectively drive the reaction toward benzoic acid while effectively suppressing the formation of byproducts like acetophenone. In 2026, Chen's group demonstrated that spent lithium manganese oxide ($LiMn_2O_4$) cathodes can be directly repurposed as heterogeneous catalysts for PS oxidation to benzoic acid [75]. The catalytic activity originates from asymmetric Mn^{3+}–O–Mn^{4+} motifs that facilitate lattice oxygen activation and $\bullet O_2^-$ generation, driving selective C–C cleavage. The optimized system achieved 89% conversion with ~70% benzoic acid selectivity at 150°C within 1 h, and effectively converted real-world PS wastes. Techno-economic analysis revealed a minimum selling price of $0.89/kg—below market value—with substantially reduced environmental footprint. This work exemplifies a dual-waste co-recycling paradigm that simultaneously valorizes spent batteries and waste plastics.

While these thermally driven pathways deliver exceptional yields and demonstrate immense potential for processing realistic, mixed-plastic feedstocks, their inherent reliance on elevated temperatures and pressurized oxygen highlights the ongoing necessity for more energy-efficient catalytic designs (Figure 14).

3.5 Photoelectrochemical and Synergistic Energy Pathways

To transcend the thermodynamic and kinetic limitations of monomodal energy inputs (e.g., purely photochemical or thermal systems), the integration of photochemistry and electrochemistry has recently emerged as a formidable frontier for polymer upcycling. This multi-energy coupling enables highly complementary activation pathways, thereby maximizing catalytic efficiency and enabling the co-generation of valuable energy carriers. In a seminal 2026 study, Ackermann's group pioneered a photo–electro–iron cooperative catalytic system for the exhaustive degradation of PS

Downloaded from https://www.cambridge.org/core. 15 Nov 2026 at 12:57:10, subject to the Cambridge Core terms of use.

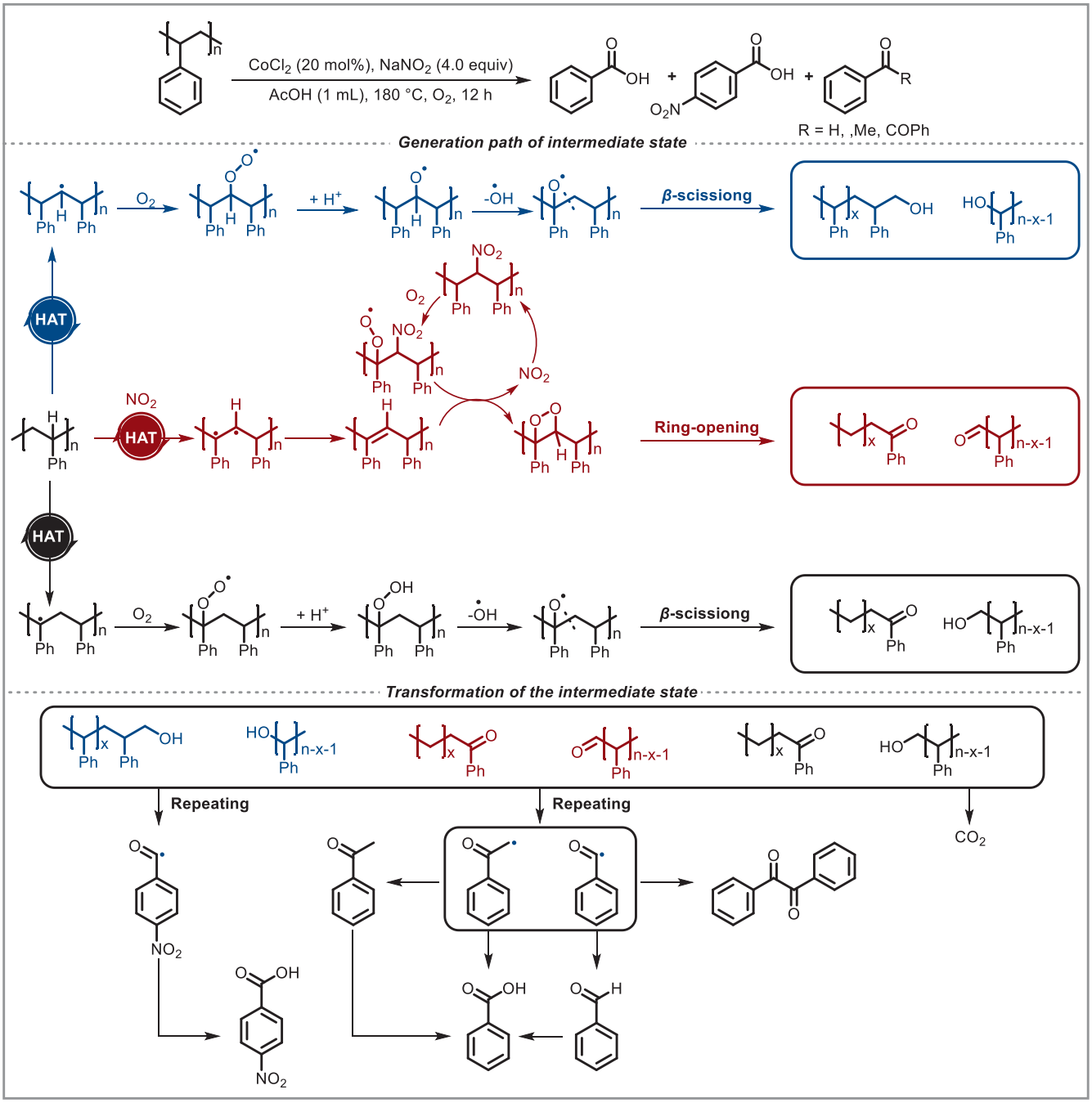


Figure 14. Mechanism of Co(II)-catalyzed oxidative degradation of polystyrene with $NaNO_2$/AcOH under oxygen. Three parallel pathways proceed via HAT, oxygen addition, and *β*-scission/ring-opening, ultimately yielding benzoic acid, nitrobenzoic acid, and other aromatic carbonyl products.

coupled with green hydrogen production [55]. Utilizing iron(III) tetraphenylporphyrin chloride as the molecular catalyst, PS was oxidatively depolymerized under synergistic 390 nm irradiation and constant-current electrolysis. Under optimized conditions, this triple-activation protocol afforded benzoyl products in an impressive total yield of up to 73.7%. Detailed mechanistic elucidations revealed a sophisticated interplay between the applied energy fields: electrochemistry primarily initiates the anodic cleavage of the polymer backbone, whereas light irradiation plays a decisive role in accelerating the subsequent deep oxidation of the oligomeric intermediates. Crucially, it was discovered that cathodic oxygen reduction generates hydrogen peroxide in situ, which subsequently reacts with the iron porphyrin to form highly reactive high-valent iron–oxo species that vigorously promote benzylic HAT. Concurrently, anodic oxidation generates benzylic radicals, perfectly paired with the cathodic hydrogen evolution reaction (HER). The robustness of this protocol was further validated by its exceptional tolerance toward real post-consumer PS wastes—readily processing commercial items contaminated with dyes, additives, and food residues (affording 44%–73% product yields). By elegantly coupling anodic waste polymer valorization with cathodic hydrogen generation, this photoelectrocatalytic paradigm charts a highly

Downloaded from https://www.cambridge.org/core. 15 Nov 2026 at 12:57:10, subject to the Cambridge Core terms of use.

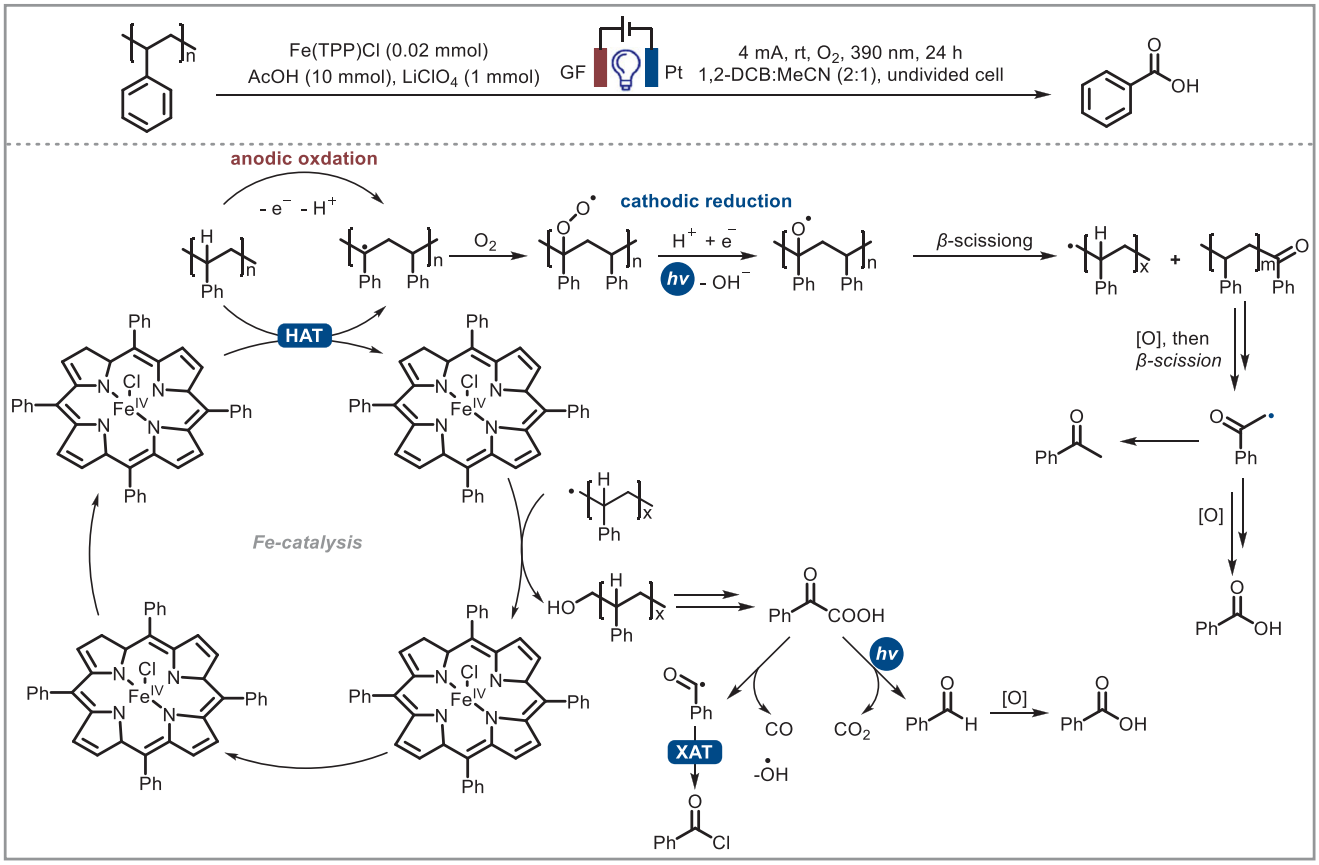


Figure 15. Mechanism of electrophotocatalytic PS degradation mediated by Fe(TPP)Cl. The process combines anodic oxidation, cathodic reduction, and Fe-catalyzed HAT, followed by oxygen addition and β-scission, to yield benzoic acid and other aromatic products.

sustainable and economically compelling trajectory for next-generation plastic upcycling (Figure 15).

3.6 Summary

The preceding subsections have surveyed diverse catalytic systems—spanning homogeneous photocatalysis, heterogeneous semiconductors, thermal oxidation, and photoelectrochemical approaches—all of which operate through a common mechanistic blueprint: benzylic C–H activation followed by oxidative C–C cleavage. Yet, as summarized in Table 2, a deeper analysis reveals fundamental distinctions across three key mechanistic dimensions. The choice between direct HAT and ROS-mediated initiation dictates the inherent selectivity–kinetics trade-off: direct HAT offers higher site selectivity through precise BDE matching, whereas ROS pathways accelerate reaction rates at the cost of indiscriminate oxidative attacks. The reaction trajectory is governed by the competition between kinetic barriers (C–H activation and β-scission) and thermodynamic driving forces (the deep exergonic well of stable oxygenate formation), which together create a thermodynamic sink that channels product distributions predominantly toward benzoic acid. Preventing over-oxidation to CO_2 requires a "kinetic pause"—ensuring that the desired products possess a higher kinetic barrier to further oxidation than the parent polymer. From a sustainability standpoint, oxidative upcycling presents a clear dichotomy. Homogeneous photocatalysis offers mechanistic tunability under mild conditions, but relies on organic solvents and faces catalyst recovery challenges. Heterogeneous systems enable facile separation yet often require elevated temperatures or pressurized O_2. Thermal oxidation delivers the highest yields and tolerates real-world impurities, but operates at 120°C–180°C under pressurized O_2 with corrosive promoters. Photoelectrochemical approaches offer ambient operation with H_2 cogeneration but remain early in development. Despite these advances, most systems remain trapped in the benzoic acid sink. Breaking this bottleneck requires a conceptual departure from direct oxidative scission—a direction explored in the following section through skeletal rearrangement and pre-functionalization strategies that bypass conventional thermodynamic preferences to access diverse high-value aromatics. Translating these fundamental protocols to real-world mixed waste streams under scalable conditions will ultimately define the success of sustainable PS upcycling.

4. Skeletal Rearrangement and Advanced Oxygenative Diversification

While Section 3 focuses on the exhaustive oxidative deconstruction of PS into primary commodity oxygenates (e.g., benzoic acid), this section addresses more advanced oxygenative trajectories that transcend conventional chain-scission pathways. By integrating catalytic skeletal rearrangements, Hock-type transformations, and pre-oxidative topological editing, these advanced strategies deliberately bypass traditional thermodynamic sinks. Rather than yielding standard benzoic acid, these protocols orchestrate precise skeletal and functional alterations to synthesize structurally diverse,

Downloaded from https://www.cambridge.org/core. 15 Nov 2026 at 12:57:10, subject to the Cambridge Core terms of use.

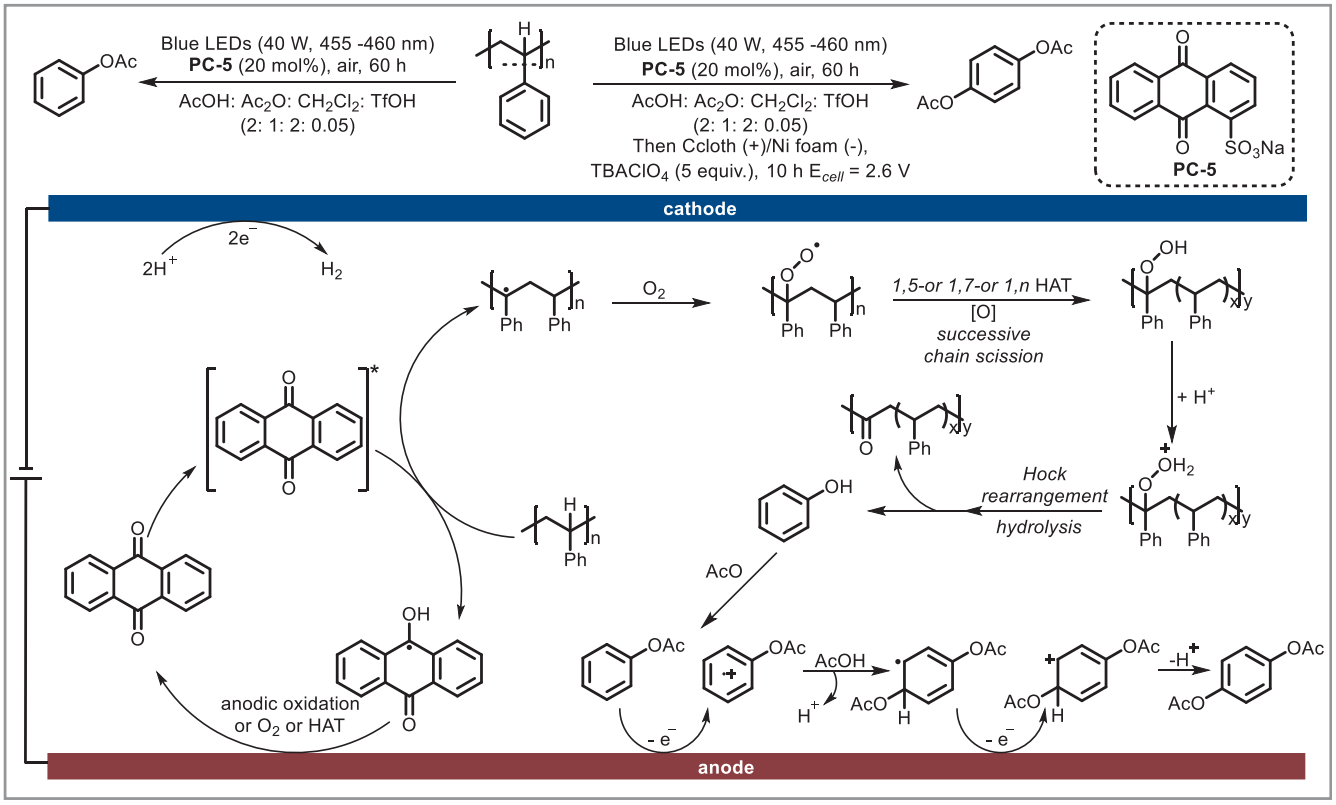


Figure 16. Photoelectrocatalytic degradation to phenol and aryl acetates via anthraquinone-mediated HAT and chain scission.

high-value oxygenated fine chemicals, such as phenols, terephthalic acid, and phthalic anhydride.

4.1 Hock-Type Rearrangement Pathways to Phenolic Compounds

The Hock rearrangement, a classical industrial route for phenol production via the acid-promoted cleavage of cumene hydroperoxide, has recently been elegantly extended to the oxidative upcycling of PS. In 2025, Stahl's group reported the first thermally driven Hock-type transformation of PS [76]. Employing an NHPI-derived HAT mediator and AIBN under 10 atm O_2, PS dimers and trimers underwent autoxidation, followed by perchloric-acid-promoted rearrangement of the resulting hydroperoxide intermediates. While the dimer afforded phenol in 30% yield, the trimer exhibited a lower yield (17%) due to steric constraints hindering oxidation at internal benzylic sites. When applied to the PS polymer, approximately 25% of benzylic positions were oxygenated, delivering phenol in a 12.7% yield alongside polymer chain scission. Almost concurrently, Shen's group developed a photocatalytic variant that circumvents the harsh thermal requirements, enabling the one-step conversion of PS into phenol derivatives under ambient conditions [77]. Utilizing sodium anthraquinone sulfonate as the photocatalyst and triflic acid to suppress competing benzoic acid pathways, PS was transformed into phenyl acetate (22% yield) under blue-light irradiation in air. This protocol involves initial benzylic hydroperoxidation, subsequent acid-catalyzed Hock rearrangement, and in situ acetylation. Notably, coupling this photochemical step with electrochemical oxidation enabled the synthesis of 1,4-diacetoxybenzene with an overall yield of 14.1% under solar-driven conditions, showcasing a highly sustainable route to diverse phenolic building blocks (Figure 16). Almost concurrently, Stache's group developed a mild photooxidative HAT strategy using Eosin Y as a metal-free photocatalyst for PS-to-phenol conversion under blue light (456 nm) at room temperature and 1 atm O_2 [78]. The reaction proceeds via benzylic C–H abstraction by photoexcited Eosin Y, followed by O_2 trapping to form hydroperoxyl PS (PS-OOH), which undergoes acid-catalyzed Hock rearrangement to afford phenol (up to 21% yield from pristine PS). Notably, this protocol was successfully applied to eight post-consumer PS plastics (including cups, lids, foams, and LEGO blocks), achieving phenol yields up to 23% after purification—comparable to the industrial cumene process. While additives such as TiO_2 and carbon black diminished yields due to light scattering/absorption, the system proved compatible with plasticizers (DEHP), flame retardants (HBCD), and processing aids ($CaSt_2$). This work establishes a mild, metal-free photocatalytic platform for converting waste PS into phenol, complementing thermal Hock strategies. Ultimately, adapting the classical Hock rearrangement to macromolecular systems marks a leap in the advanced upcycling of PS. By circumventing unselective fragmentation via targeted benzylic oxygenation and skeletal rearrangement, these methodologies unlock a direct pathway to high-value phenols, elegantly bridging plastic waste valorization with mainstream industrial synthesis.

4.2 Tandem Electrophilic Functionalization and Oxidative Cleavage

Beyond phenol production, another compelling alternative strategy involves functionalizing the aromatic backbone prior to oxidative deconstruction, enabling access to high-value aromatic

Downloaded from https://www.cambridge.org/core. 15 Nov 2026 at 12:57:10, subject to the Cambridge Core terms of use.

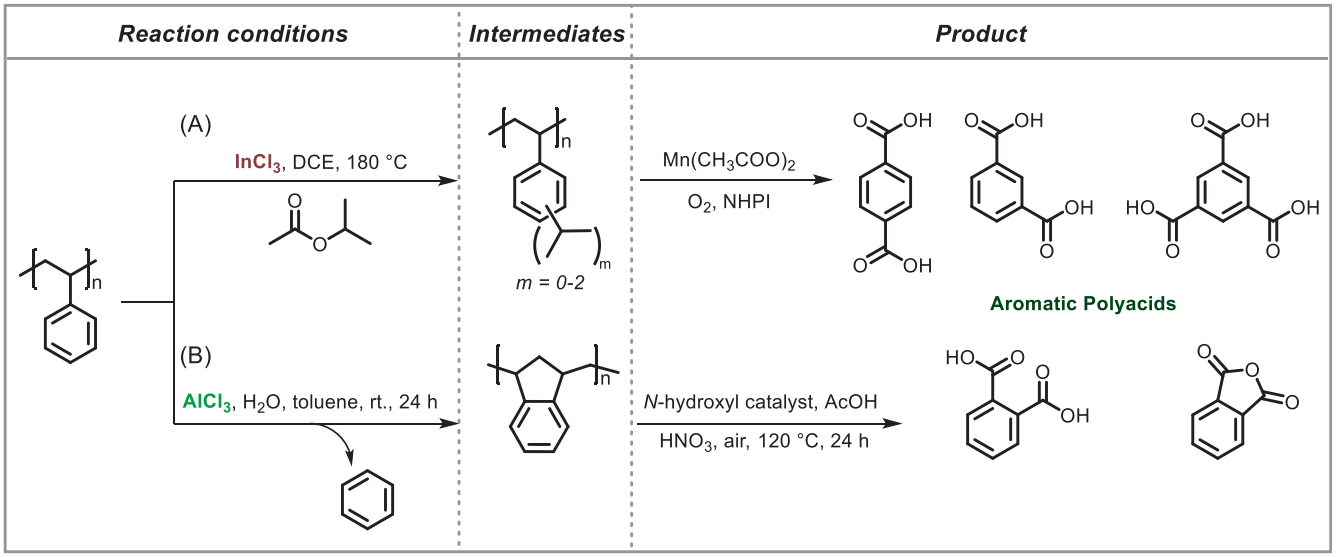


Figure 17. (a) Lewis acid-catalyzed functionalization and oxidation to aromatic carboxylic acids. (b) $AlCl_3$-catalyzed rearrangement to polyindane, followed by oxidation to phthalic acid derivatives.

polycarboxylic acids. In 2024, De Vos's group reported a tandem strategy integrating Friedel-Crafts functionalization with oxidative degradation [79]. In this sequence, PS phenyl rings were initially modified via either acylation or alkylation, and subsequently oxidatively cleaved to yield terephthalic acid (TA), isophthalic acid, and trimesic acid. In the acylation route, $AlCl_3$ and acetic anhydride achieved nearly quantitative para-acylation of the PS rings, delivering TA in an isolated yield of 55 mol% after oxidation. Alternatively, an alkylation route catalyzed by $InCl_3$ (6 mol%) with isopropyl acetate achieved ~60% polymer functionalization, yielding a mixture of TA, isophthalic acid, and benzoic acid. Impressively, the obtained TA could be directly esterified to dimethyl terephthalate (97% purity) and repolymerized into virgin PET, demonstrating a remarkable closed-loop upcycling trajectory from waste PS to high-performance PET (Figure 17a). Ultimately, this ingenious pre-functionalization sequence elegantly illustrates how macromolecular editing prior to cleavage can fundamentally reroute degradation pathways, establishing a formidable "cross-polymer" upcycling bridge between distinct commodity plastic value chains.

4.3 Skeletal Rearrangement to Ortho-Functionalized Aromatics

The intrinsic steric hindrance of the PS backbone dictates that direct electrophilic substitutions predominantly occur at the para-position. In a remarkable departure from this paradigm, Lim's group reported in 2025 the first conversion of PS into 1,2-disubstituted aromatics (e.g., phthalic anhydride) via a macro-to-micro skeletal rearrangement strategy [56]. Using $AlCl_3$ at room temperature, PS underwent skeletal reorganization to form polyindane (73% conversion). This polyindane intermediate was subsequently oxidized in an $AcOH/HNO_3$ system at 100°C, utilizing N-hydroxy catalysts (THICA or NHPI) to afford phthalic acid and phthalic anhydride. Mechanistically, this ingenious sequence proceeds via protonation of the phenyl ring and subsequent phenyl abstraction to form carbocations, which undergo intramolecular cyclization to circumvent the native spatial constraints. Demonstrated on a 10 g scale with mixed PS wastes, this protocol yields phthalic anhydride that can be readily purified via sublimation and further derivatized into premium fine chemicals like fluorescein and phenolphthalein (Figure 17b). By rewriting the polymer's topology prior to cleavage, this macro-to-micro indanization elegantly bypasses polystyrene's spatial limitations, unlocking new chemical space for fine chemical synthesis.

4.4 Summary

Overall, recent breakthroughs underscore that the chemical space accessible from PS waste can be significantly expanded beyond rudimentary aromatic monomers through versatile upgrading strategies. By harnessing Hock-type rearrangements, tandem Friedel-Crafts functionalizations, and pre-oxidative skeletal reorganizations, researchers have successfully bypassed thermodynamic sinks to synthesize structurally diverse, high-value aromatics (e.g., phenols, terephthalic acid, and phthalic anhydride). Nevertheless, these advanced synthetic cascades frequently suffer from multi-step complexities and rely heavily on stoichiometric or highly corrosive reagents (e.g., $AlCl_3$, HNO_3, perchloric acid). Consequently, future innovations must focus on developing robust, multifunctional, and benign catalytic systems capable of orchestrating these multi-pathway transformations in a more streamlined, one-pot fashion. Sustainability-wise, these advanced routes unlock products with significantly higher market value than benzoic acid, but at the cost of multi-step complexity and stoichiometric corrosive reagents ($AlCl_3$, HNO_3). $AlCl_3$ generates substantial aluminum waste, while HNO_3 produces NO_x emissions. Carbon efficiency is higher than exhaustive oxidation, yet cumulative losses at each step remain a concern. Future work should prioritize one-pot tandem systems to minimize intermediate purification.

5. Structural Diversification via Heteroatom Incorporation

Moving beyond traditional oxygenative pathways, the strategic incorporation of nitrogen and sulfur represents a highly rewarding frontier in PS upcycling. Because N/S-heteroaromatics are

Downloaded from https://www.cambridge.org/core. 15 Nov 2026 at 12:57:10, subject to the Cambridge Core terms of use.

indispensable building blocks in pharmaceuticals and advanced materials, directly transforming inert plastic waste into these intricate structures vastly expands the accessible chemical space [80,81].

5.1 Nitridative Scission and Oxidative Amination Pathways

The direct insertion of nitrogen atoms into the robust non-polar backbone of polyolefins poses distinct thermodynamic challenges. In 2024, Jiao's group reported a pioneering nitridative scission strategy, enabling the conversion of diverse polyolefin wastes (including PS) into nitriles and amides [68]. Utilizing MnO_2 as the catalyst and urea as a ubiquitous nitrogen source under an oxygen atmosphere (200°C, 15 bar O_2), PS was selectively converted into benzonitrile and benzamide. Detailed kinetic profiling revealed that the cascade is initiated by the rapid chain scission of PS to form amide-terminated oligomers, which subsequently undergo deep oxidation. Impressively, this protocol was successfully applied to discarded LEGO bricks (yielding 2.84 g of *N*-containing products) and various styrenic copolymers (SBS, ABS, HIPS). Subsequently, in 2025, the Huang's group developed an alternative nitridative degradation paradigm leveraging a CuBr catalyst with acetonitrile acting dually as the nitrogen source and solvent [57]. Under 200°C and 2 MPa O_2, commercial PS was converted to benzonitrile and benzamide in a combined yield of 70%. Mechanistic elucidations highlighted that a trace amount of water (40 μL) acts as a crucial promoter, triggering the formation of hydroxyl radicals that facilitate the thermal decomposition of acetonitrile to release in situ ammonia. Notably, the homogeneous CuBr catalyst undergoes a phase transition into a recoverable heterogeneous solid during the reaction, enabling excellent recyclability. While these oxidative amination strategies achieve unprecedented skeletal functionalization, their ubiquitous reliance on extreme thermobaric conditions (e.g., 200°C, 15–20 bar O_2) and aggressive oxidative environments highlights the pressing need to develop lower-energy catalytic alternatives (Figure 18a). Nevertheless, by successfully breaching the formidable thermodynamic barriers of direct nitrogen incorporation, these pioneering methodologies fundamentally expand the chemical space of polymer deconstruction, providing a powerful blueprint for the direct transformation of inert plastics into high-value, heteroatom-functionalized chemical portfolios.

5.2 Sulfur-Mediated Radical Cascades and Tandem Sulfenylation

Paralleling the advancements in nitrogen incorporation, the targeted installation of sulfur atoms into the PS backbone has unlocked new avenues for producing valuable organosulfur building blocks. In 2023, Liu's group [82] designed a sophisticated tandem "degradation-upgrading" cascade. Initially, PS was exhaustively unzipped into benzene (97.6% yield) via an $AlCl_3$-catalyzed random chain-scission mechanism. This in situ generated benzene subsequently served as a platform intermediate, undergoing consecutive Friedel–Crafts reactions with various acyl chlorides or thionyl chloride ($SOCl_2$). Remarkably, when $SOCl_2$ was employed, polycyclic aromatic hydrocarbons (e.g., naphthalene) concurrently formed during degradation served as in situ hydrogen donors via a Scholl reaction, driving the highly selective reduction of sulfoxide intermediates to diphenyl sulfide (88% selectivity).

More recently, in 2025, Chen's group demonstrated a brilliant solar-driven photothermal co-upcycling strategy, utilizing elemental sulfur (S_8) dually as a photothermal susceptor and a reactant [83]. By concentrating sunlight via a concave mirror under solvent-free conditions, the PS/S_8 mixture rapidly achieved localized temperatures exceeding 450°C, driving the reaction to completion within mere minutes to afford 2,4-diphenylthiophene and 1,3,5-triphenylbenzene. DFT calculations and trapping experiments confirmed that photothermally generated sulfur radicals abstract hydrogen atoms from PS to yield alkene intermediates, which then undergo thermodynamically favored radical addition and cyclization. Although these sulfur-incorporation cascades ingeniously bypass traditional oxidative sinks, the necessity for highly corrosive Lewis acids ($AlCl_3$, $SOCl_2$) in tandem pathways or extreme localized heating in photothermal designs presents significant engineering hurdles for continuous, large-scale processing (Figure 18b). Nevertheless, by unlocking direct access to complex organosulfur architectures, these pathways significantly broaden the versatile upcycling portfolio of polystyrene.

5.3 Summary

In summary, directly constructing C–N and C–S bonds onto inert PS backbones marks a conceptual breakthrough, elevating plastic upcycling from rudimentary oxidative deconstruction to the targeted synthesis of high-value heteroaromatics (e.g., nitriles, amides, thiophenes). By orchestrating radical cascades, nitridative scissions, and photothermal cyclizations, researchers have successfully breached the severe thermodynamic barriers of C–H/C–C functionalization. However, this nascent field remains confined by harsh operational windows, relying heavily on hyperbaric oxygen, extreme temperatures, and corrosive reagents. Designing robust catalytic microenvironments capable of operating under mild conditions to circumvent these limitations is crucial for broad industrial implementation. The sustainability tension here is acute: nitrogen/sulfur-containing aromatics command premium prices, but their synthesis requires exceptionally harsh conditions (200°C, 15–20 bar O_2) or stoichiometric corrosive reagents. Energy inputs rank among the highest of all PS upcycling strategies. While homogeneous-to-heterogeneous catalyst recovery in the CuBr/acetonitrile system is promising, it remains laboratory-scale. Future efforts must focus on earth-abundant heterogeneous catalysts operating under significantly milder conditions.

6. Precision Grafting Modification to Advanced Polymer Materials

Distinguishing skeleton retention from backbone cleavage: a strategic comparison. Before delving into specific methodologies, it is imperative to establish a clear conceptual distinction between the two fundamental paradigms of PS upcycling. Catalytic deconstruction ("Breaking the Backbone") relies on exhaustive fragmentation of the C(sp^3)–C(sp^3) backbone to recover monomers or yield small-molecule oxygenates, a process that inherently destroys the macromolecular architecture. In contrast, precision grafting modification ("re-using the skeleton") selectively targets the pendant phenyl rings or benzylic C–H bonds without triggering β-scission, thereby preserving the polymer backbone while introducing functional groups that confer new properties. The hallmark of advanced grafting lies in its precision: achieving high regioselectivity (e.g., para-functionalization of the phenyl ring), controlling the degree of substitution, and strictly avoiding undesired cross-linking or uncontrolled chain degradation. This precise macromolecular

Downloaded from https://www.cambridge.org/core. 15 Nov 2026 at 12:57:10, subject to the Cambridge Core terms of use.

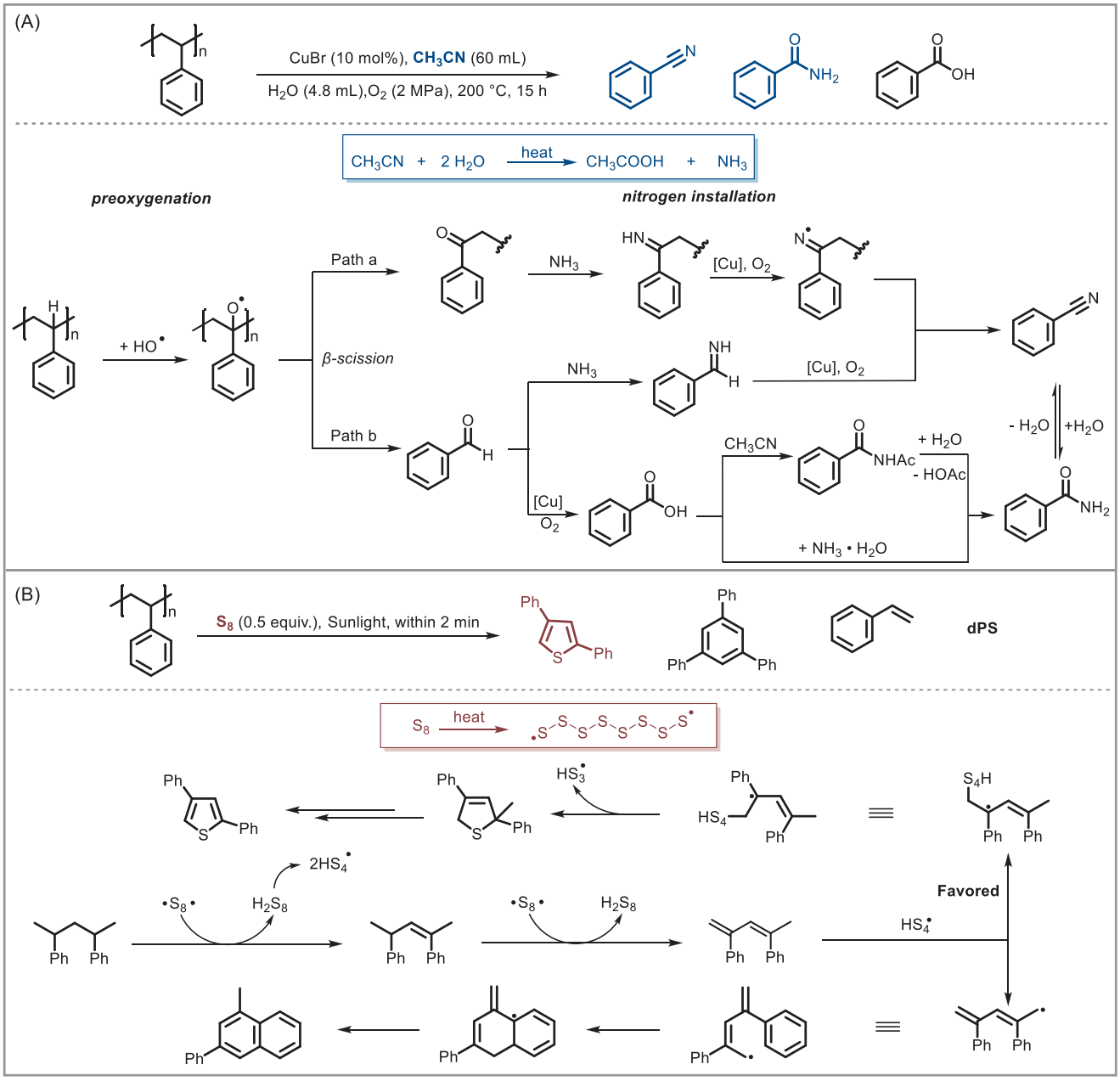


Figure 18. (a) Mechanism of CuBr-catalyzed conversion of PS to benzonitrile and benzamide. (b) Sulfur-mediated radical cascades and tandem sulfenylation in sunlight-driven PS degradation.

editing transforms waste PS into high-value functional materials—polyelectrolytes, adsorbents, or conductive matrices—without falling into the thermodynamic sinks of complete chain breakdown. Strategically, skeleton retention offers a low-energy alternative to total depolymerization, particularly when the goal is to maximize carbon retention and generate high-value specialty materials, provided that the inherent complexities of real-world waste feedstocks can be effectively managed.

To guide readers through the comparative landscape of these two paradigms, we present below a systematic assessment across four critical dimensions—product value, energy consumption, carbon efficiency, and overall sustainability (Table 3).

6.1 Photo-Mediated C(Sp^2)–H Functionalization and Graft Initiation

Directly editing the inert aromatic rings of PS without inducing backbone degradation requires exquisite catalytic control. In a pioneering example, Leibfarth's group reported a photoredox C (sp^2)–H functionalization strategy leveraging electrophilic fluoroalkyl radicals for the precise post-polymerization modification of PS [58]. Utilizing $Ru(bpy)_3Cl_2$ as the photocatalyst, paired with pyridine *N*-oxide and trifluoroacetic anhydride, this system successfully transfigured native aromatic C–H bonds into trifluoromethylated units under ambient blue-light irradiation. The functionalization density could be precisely tuned (19–

Downloaded from https://www.cambridge.org/core. 15 Nov 2026 at 12:57:10, subject to the Cambridge Core terms of use.

Table 3. Comparison of "breaking the backbone" and "re-using the skeleton" strategies for PS upcycling.

Dimension	Breaking the backbone	Re-using the skeleton
Product type	Small molecules (monomers, aromatics, oxygenates)	Functional polymers (materials)
Product value	Low–moderate ($1.5–5/kg)	High (>$10/kg for specialty materials)
Market volume	Large (commodity scale)	Small-moderate (niche applications)
Energy input	High (often >150°C)	Low (RT to 80°C)
Carbon efficiency	Moderate–low (carbon loss to CO2)	High (complete carbon retention)
Waste tolerance	Variable (additives cause deactivation)	Moderate(depends on functionalization method)
Technology readiness	High (pyrolysis industrially established)	Low-moderate (emerging)
Best application	Clean PS streams, closed-loop monomer recovery	Contaminated streams, high-value material production

71 mol%) by modulating reagent stoichiometry. Crucially, GPC confirmed that the polymer's molecular weight distribution remained remarkably intact, validating the complete suppression of deleterious chain-scission or cross-coupling pathways. While ^{19}F NMR indicated a statistical distribution of modifications primarily at the para and meta positions, the protocol exhibited exceptional robustness across diverse aromatic polymers (e.g., PET, polycarbonate) and post-consumer EPS foams. Most notably for macromolecular engineering, substituting the reagent with bromodifluoroacetic anhydride introduced bromodifluoromethyl handles (15 mol%) directly onto the PS backbone. These dormant halide sites function as highly efficient macroinitiators for subsequent atom transfer radical polymerization (ATRP), seamlessly enabling the "grafting-from" synthesis of complex PS-graft-polyacrylate architectures. While highly precise, this protocol's reliance on expensive precious metal catalysts (Ru) and specialized fluorinated reagents limits its scalability. Future efforts must prioritize earth-abundant, cost-effective catalytic systems for practical upcycling (Figure 19a). Ultimately, by demonstrating the feasibility of non-destructive structural editing, this approach redefines waste polystyrene as a highly versatile macromolecular scaffold for advanced materials engineering.

6.2 Transition-Metal-Catalyzed C(sp^2)–H Activation and Late-Stage Diversification

Transition-metal catalysis offers a powerful toolkit for the site-selective functionalization of aromatic C–H bonds, allowing for the installation of versatile functional handles without compromising the polymer backbone. In 2023, Wang's group reported a seminal $AuCl_3$-catalyzed, para-selective bromination of PS C(sp^2)–H bonds using NBS under mild conditions (40°C) [84]. By modulating the NBS stoichiometry, the bromination density could be precisely tuned (24–93 mol%) while rigorously maintaining the pristine molecular weight distribution—confirming the absence of deleterious chain scission or cross-linking. Crucially, the resulting brominated PS functioned as a versatile macromolecular scaffold for late-stage diversification via cross-coupling cascades (e.g., Suzuki, Heck, and Sonogashira). This enabled the modular introduction of amino, boronate, aryl, and alkenyl moieties, thereby affording precise control over the polymer's thermal properties (elevating the glass transition temperature, T_g, from 99°C to 135°C) and surface wettability (Figure 19b).

Extending this precision engineering to heteroatom functionalization, in 2024, Shen's group developed an earth-abundant manganese-catalyzed strategy for the direct phosphonation of PS to fabricate advanced flame-retardant materials [85]. Utilizing inexpensive $Mn(OAc)_2$ and phosphites in DMF (80°C), phosphonate groups were covalently grafted onto the aromatic rings via robust C–P bonds. GPC verified the exceptional preservation of the polymer architecture during this modification (6.8–13.6 mol% functionalization). Macroscopically, this targeted grafting profoundly enhanced the material's thermal stability: the modified polymer exhibited a nearly six-fold increase in char yield (from 2.48% to 14.44%), alongside a ~40% reduction in both peak heat release rate (*p*HRR) and heat release capacity (HRC). Notably, this protocol demonstrated excellent applicability to real-world plastic wastes, including foamed PS and SAN copolymers (Figure 19c). Extending the Au-catalyzed bromination platform, in 2026, Skrydstrup's group developed a two-step protocol for converting PS into amine-functionalized CO_2 adsorbents [86]. PS-Br with tunable bromination degrees (11%–93%) was subjected to Cu-catalyzed Ullmann-type amination with aliphatic diamines (EDA, TAEA), yielding macroporous solid sorbents with CO_2 capacities up to 2.5 mmol g^{-1} at 25°C (0.77 mmol g^{-1} under DAC conditions). The protocol was validated on five real-world PS wastes and, notably, the amine source could be derived from depolymerized polyurethane waste—enabling a closed-loop upcycling paradigm. Solid-state NMR revealed carbamate/carbamic acid formation at primary amine sites as the primary adsorption mechanism. This work demonstrates the translation of precision C–H functionalization into functional materials for environmental applications, bridging plastic upcycling with carbon capture.

Transition-metal-catalyzed C–H activation provides unmatched regioselectivity and enables sophisticated late-stage macromolecular diversification. However, the rigorous removal of trace transition metal residues—which can detrimentally alter the long-term optical, electrical, and degradation properties of the functionalized polymers-remains a critical purification hurdle that must be addressed before large-scale industrial translation.

6.3 Electrochemical Modification: From Dearomatization to C–H Functionalization

Harnessing the electron as a traceless reagent, electrochemical C–H functionalization offers a highly sustainable, reagent-economical paradigm for precision macromolecular engineering. In 2021, Sarlah's group reported the first systematic investigation into the electroreductive dearomatization of PS [87]. Using a constant current electrolysis setup with LiBr as electrolyte and HMPA as additive in THF, the aromatic rings of PS were selectively reduced to 1,4-cyclohexadiene moieties, delivering poly(vinylcyclohexadiene) (PVCHD). Remarkably, the degree of reduction could be precisely tuned (0%–100%) by adjusting the charge passed (1.0–6.0 F mol^{-1}), and the transformation proceeded without significant chain scission or cross-linking across a wide molecular weight range (10^3–10^6 Da). The dearomatized products serve as versatile platforms for downstream olefin chemistry: chemoselective reduction with diimide yielded

Downloaded from https://www.cambridge.org/core. 15 Nov 2026 at 12:57:10, subject to the Cambridge Core terms of use.

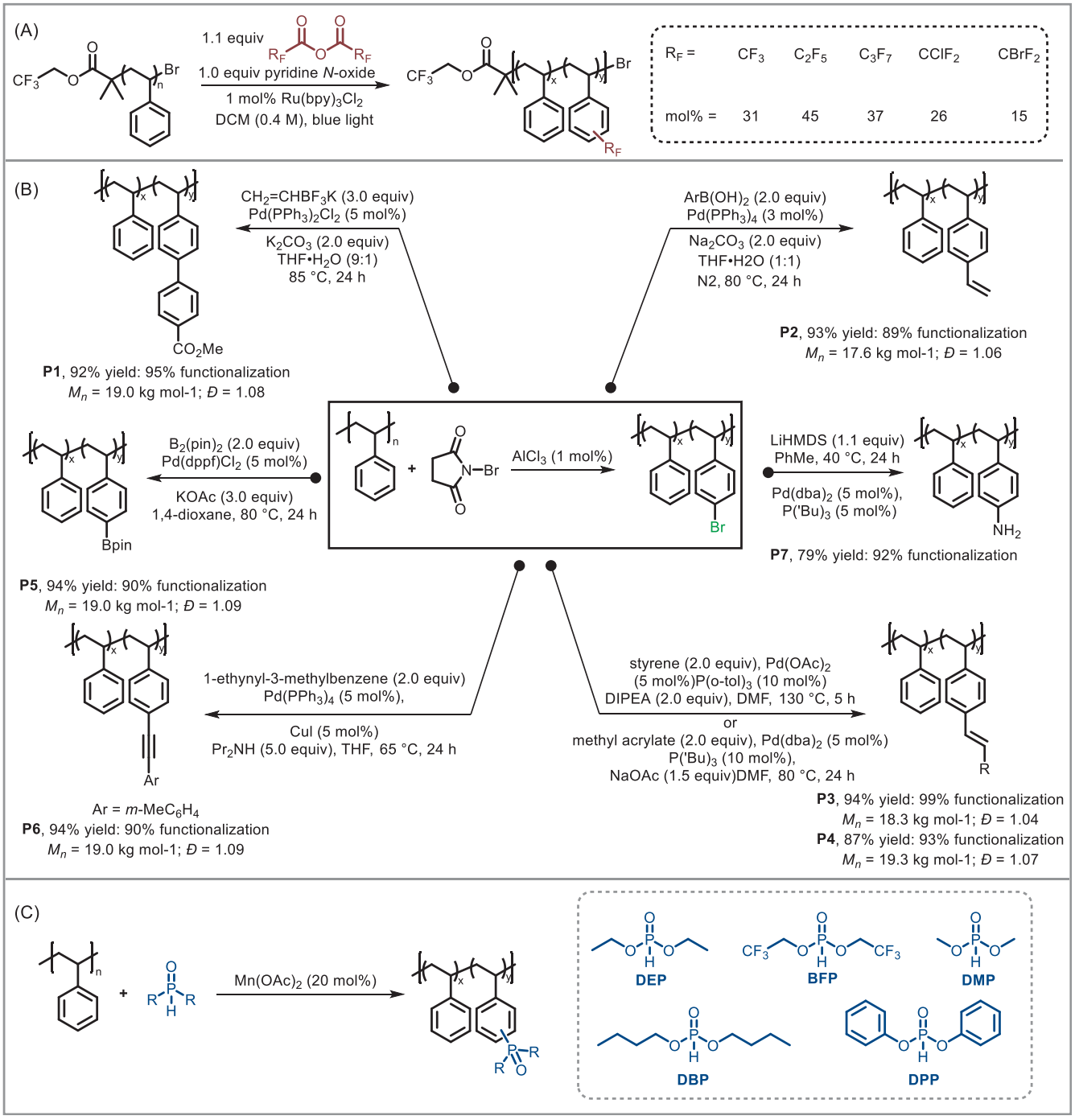


Figure 19. Site-selective C–H functionalization of PS: (a) Photochemical bromination with fluorinated reagents. (b) Modular cross-coupling reactions (Suzuki, Heck, Sonogashira, borylation, and C–N coupling) using the brominated polymer. (c) Direct Mn-catalyzed C–H phosphonylation with various phosphite reagents.

poly(vinylcyclohexene), while epoxidation with mCPBA afforded epoxidized materials with tunable glass transition temperatures (up to 162°C)—functionalized polymers that would be challenging to prepare by any other means. The practicality of this approach was demonstrated on a 20 g scale and on commercial foam cups. This work established electrochemistry as a powerful tool for accessing novel polymer architectures through dearomatization. In 2025, Naumann's group reported an innovative electro-oxidative platform for the late-stage thianthrenation of PS [88]. Through the anodic oxidation of TA at a graphite electrode, highly reactive TA radical cations are generated, which subsequently undergo targeted cross-coupling with the benzylic aromatic rings to yield rigid thianthrenium salt polyelectrolytes. By modulating the TA-to-PS feed ratio, the degree of functionalization (DF) was precisely tuned from 18% to 87% without inducing backbone cleavage, maintaining the polymer's pristine molecular weight distribution. This platform proved highly robust, accommodating high-molecular-weight EPS waste and

Downloaded from https://www.cambridge.org/core. 15 Nov 2026 at 12:57:10, subject to the Cambridge Core terms of use.

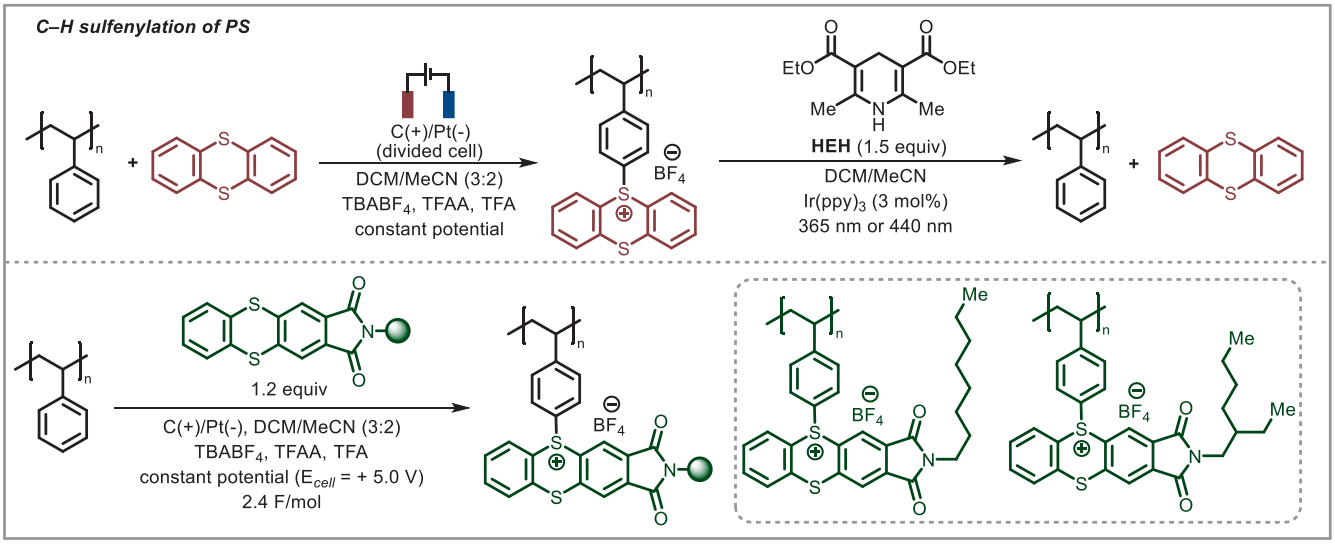


Figure 20. Electrochemical and photoredox-mediated C–H sulfenylation of PS with phenothiazine derivatives.

various TA derivatives bearing carboxyl, imide, and ester moieties (DF 59%–79%). The resulting cationic polyelectrolytes displayed unique phase separation and crystallization behaviors, and successfully functioned as macromolecular photoacid generators for epoxy curing. Most remarkably, this functionalization is dynamically reversible: under photoredox conditions, the thianthrenium handles undergo facile reductive elimination, enabling the traceless recovery of the original PS architecture with an 83% isolated yield and >99% defunctionalization (Figure 20).

While electrochemical thianthrenation offers an elegant, closed-loop approach to reversible macromolecular engineering, the inherent insulating nature of PS and the sluggish mass transport of massive polymer coils to the electrode surface present severe kinetic bottlenecks, necessitating advanced flow-cell reactor designs for future industrial scale-up.

6.4 Mechanochemical Post-Polymerization Modification

Mechanochemistry has emerged as a compelling, solvent-minimized paradigm for macromolecular engineering, utilizing mechanical force rather than thermal energy to drive transformations. In 2018, Kim's group established the viability of this approach by demonstrating a solvent-free, ball-milling-enabled Schiff-base condensation on aldehyde-functionalized PS [89]. Operating at 30 Hz for 30–60 min, the protocol achieved quantitative imine formation while strictly preserving the molecular weight distribution, proving highly selective even in block copolymers.

Advancing from pre-installed functional handles to the direct activation of inert C(sp^2)–H bonds, in 2024, Golder's group reported an elegant liquid-assisted grinding (LAG) strategy for the catalytic trifluoromethylation of commercial PS [90]. To circumvent the ubiquitous issue of mechanically induced chain scission, trace amounts of solvent (0.2–1.2 μL mg^{-1}) were introduced. This LAG approach effectively plasticized the polymer matrix, dissipating destructive mechanical energy and thereby preserving the macromolecular architecture of high-molecular-weight PS (M_n approx 26 kDa) while achieving 0.6–1.2 mol% functionalization. Remarkably, intrinsic additives in post-consumer waste (e.g., EPS foams and colored cup lids) acted as endogenous plasticizers, further suppressing chain degradation (Figure 21a).

In a parallel breakthrough involving extreme structural remodeling, in 2024, Peterson demonstrated an ultrafast mechanochemical Birch reduction of PS using a Li/ethylenediamine (EDA) system [91]. Within just one minute of milling in air, the inert aromatic rings were dearomatized into reactive skipped-diene motifs (up to 96% conversion) without significant backbone cleavage or crosslinking. Mechanistic insights revealed that THF acts as a crucial ligand to facilitate electron transfer rather than a bulk solvent. The resulting skipped-diene polymers serve as highly reactive platforms,

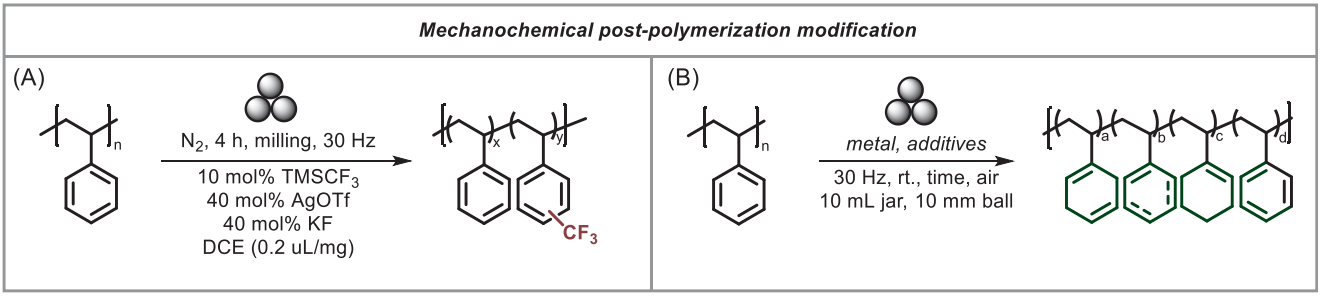


Figure 21. Materialization transformation: Functionalized and crosslinked PS. (a) Mechanochemical trifluoromethylation of brominated PS. (b) Mechanochemical crosslinking of PS using metal additives.

Downloaded from https://www.cambridge.org/core. 15 Nov 2026 at 12:57:10, subject to the Cambridge Core terms of use.

readily undergoing thiol–ene click chemistry to yield flexible, swellable polymer networks (Figure 21b).

While mechanochemical functionalization provides remarkably rapid, green, and waste-compatible routes for polymer upgrading, the inherent competition between targeted bond formation and deleterious mechanical chain-tearing remains a fundamental challenge. Furthermore, transitioning these processes from batch ball-milling to continuous twin-screw extrusion will be pivotal for the industrial realization of scalable mechanochemical upcycling.

6.5 Summary

Collectively, precision macromolecular grafting offers a thermodynamically elegant alternative to total depolymerization. By harnessing orthogonal activation modalities-spanning photoredox, transition-metal, electro-oxidative, and mechanochemical pathways—researchers can execute surgical C–H bond editing while strictly preserving the polymer's structural integrity. This enables the controlled installation of diverse chemical handles, seamlessly transforming inert PS waste into versatile platforms for late-stage diversification and advanced material fabrication. Despite these conceptual leaps, the field faces formidable translational bottlenecks. Current protocols are constrained by expensive reagents, trace transition-metal residues, sluggish mass transport, and mechanically induced chain-tearing. To overcome these hurdles, future trajectories must prioritize earth-abundant catalysts and transition from batch processing to scalable continuous-flow or twin-screw extrusion architectures, ultimately merging precision functionalization with rational materials engineering. From a sustainability perspective, grafting offers unique advantages: complete carbon retention and low energy input (room temperature to 80°C). However, product markets for functionalized polymers are smaller than those for bulk monomers, limiting waste volume absorption. Reliance on precious metals (Ru, Au) raises cost concerns, though Mn-catalyzed phosphonation offers a more abundant alternative. Heteroatom introduction may complicate end-of-life disposal. Nonetheless, grafting remains a strategically important complement to deconstruction, particularly for PS streams too contaminated for monomer recovery.

7. Materialization Transformation: Porous Carbon and Functional Materials

Beyond molecular-level editing, exploiting the inherently high carbon density and abundant aromatic pendant groups of PS provides a powerful pathway to construct macroscopic functional architectures. Through targeted processing-including pyrolytic carbonization, Friedel–Crafts hypercrosslinking, and mechanochemically driven chain extension—the linear PS framework is systematically re-engineered into robust three-dimensional networks. This material-centric trajectory directly converts end-of-life PS into high-value bulk products, such as hierarchical porous carbons for energy storage, luminescent optoelectronic films, and high-performance volatile organic compound adsorbents, offering a scientifically efficient approach for cross-disciplinary upcycling.

7.1 Porous Carbon Materials for Supercapacitor Electrodes

In 2020, Xiao's group reported a template-directed carbonization and activation strategy to upcycle waste PS into hierarchical porous carbon nanosheets for high-performance supercapacitors [59]. Utilizing porous MgO as a structural template, PS was first pyrolyzed at 700°C (34.1% yield), followed by KOH activation (700°C–900°C) to sculpt a hierarchical micro/mesoporous architecture (ACNS-X). The optimized material (ACNS-800) exhibited an extraordinary specific surface area of 2650 $m^2\ g^{-1}$, a vast pore volume of 2.43 $cm^3\ g^{-1}$, and an intrinsic oxygen doping level of 14.97 at%. This synergistic combination of an immense surface area and heteroatom doping significantly enhanced the electrochemical kinetics. In a 6 M KOH aqueous electrolyte, ACNS-800 delivered a high specific capacitance of 323 F g^{-1} at 0.5 A g^{-1}, excellent rate capability (222 F g^{-1} at 20 A g^{-1}), and 92.6% capacitance retention over 10,000 cycles. Furthermore, a symmetric supercapacitor assembled with an $EMIMBF_4$/PC organic electrolyte achieved a remarkable energy density of 44.1 Wh kg^{-1} at a power density of 757.1 W kg^{-1}, retaining 81.5% of its initial capacitance after 10,000 cycles. This work establishes a highly viable trajectory for converting carbon-rich PS waste into premium energy storage scaffolds (Figure 22a).

7.2 Optoelectronic Functional Materials: Blue-Emitting LED Films

Expanding the horizon of polymer upcycling into solid-state lighting, in 2023, Liu's group showcased an elegant strategy to transform waste expanded polystyrene (EPS) into blue-emitting luminescent matrices [92]. Following standard purification, the inert PS backbone was chemically activated via para-selective chloromethylation. These newly installed electrophilic handles served as reactive sites for the covalent grafting of 2-(2-pyridyl)benzimidazole chromophores. This targeted side-chain engineering endowed the resulting polymer (PS-PBI) with tailored photophysical properties. The PS-PBI film exhibited an excitation maximum at 356 nm—ideally overlapping with commercial 365 nm near-UV chips—and delivered a strong blue emission centered at 468 nm. Demonstrating its macroscopic utility in advanced device fabrication, the PS-PBI film was seamlessly integrated with a Eu^{3+}-complex red-emitting film and a Tb^{3+}-complex green-emitting film onto a single 365 nm UV chip. This modular assembly successfully yielded a high-performance white LED device with an exceptional color rendering index (CRI) of 93.6, underscoring a lucrative and highly innovative pathway from everyday plastic packaging to advanced optoelectronic devices.

7.3 Porous Adsorbent Materials for Environmental Remediation

Leveraging the high density of aromatic rings inherent to PS, in 2025, Xiao's group developed a Friedel-Crafts hypercrosslinking strategy to upcycle waste EPS into high-performance porous adsorbents [93]. Utilizing $FeCl_3$ as the catalyst and formaldehyde dimethyl acetal (FDA) as an external crosslinker in dichloroethane (DCE), the linear PS chains were spatially knitted into a methylene-bridged hierarchical micro/mesoporous network (PREPS-FDA/DCE). This profound structural reconfiguration yielded a remarkable BET specific surface area of 1021 m^2/g, vastly outperforming networks crosslinked solely by the DCE solvent (373 m^2/g), as structurally corroborated by solid-state ^{13}C NMR and FTIR analyses. Functionally, the abundant aromatic nodes within this rigid network engendered a highly hydrophobic, pi-electron-rich microenvironment. Consequently, PREPS-FDA/DCE exhibited exceptional uptake capacities for aromatic volatile organic compounds (VOCs)—reaching 537 mg g^{-1} for xylene and 470 mg g^{-1} for toluene—driven primarily by robust *pi–pi*

Downloaded from https://www.cambridge.org/core. 15 Nov 2026 at 12:57:10, subject to the Cambridge Core terms of use.

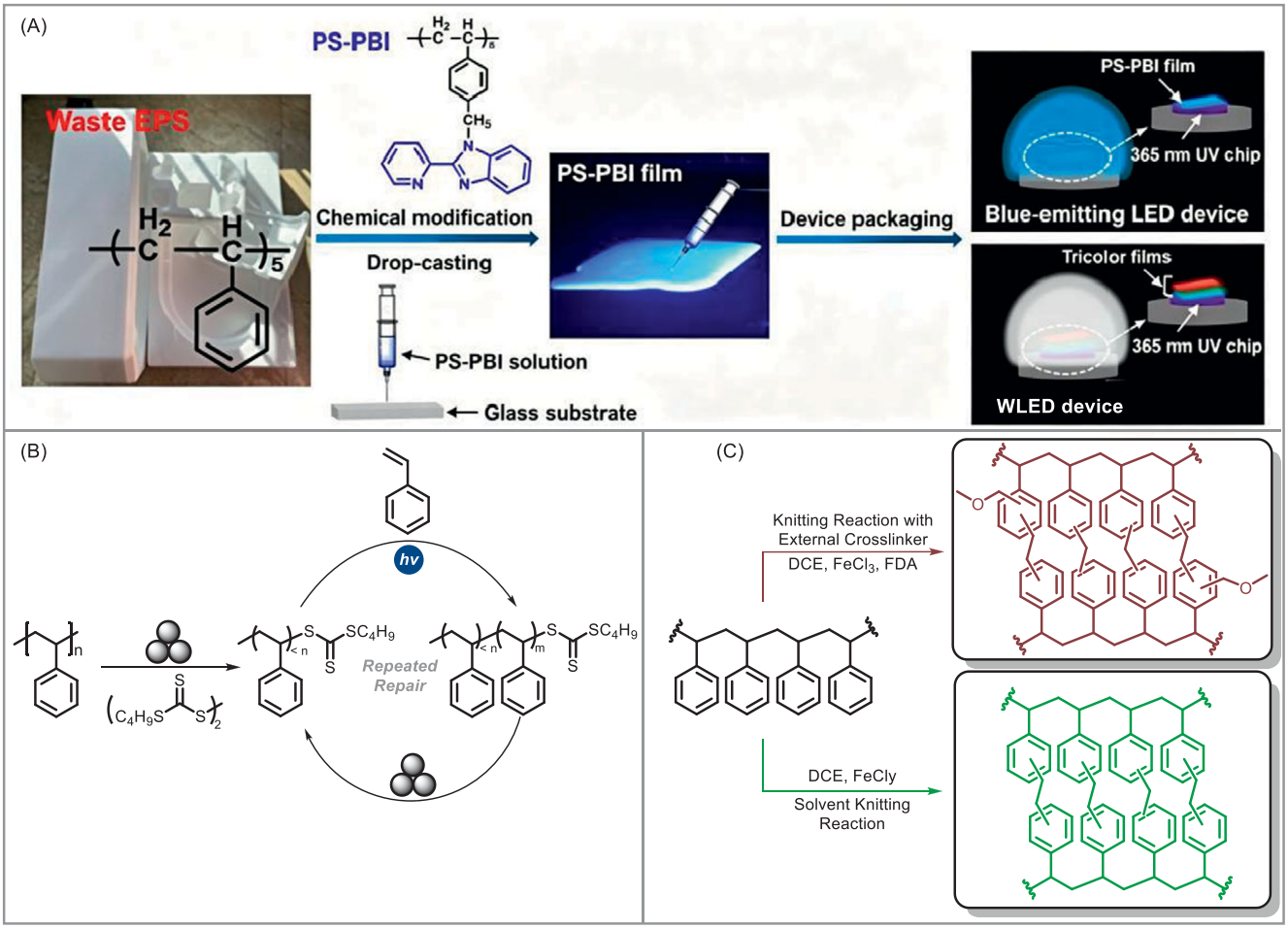


Figure 22. Porous carbon and functional materials: (a) Chemical modification to PS-PBI for blue-emitting LED and WLED device packaging. (b) Reversible RAFT-based repair of PS. (c) $FeCl_3$-mediated knitting of PS into crosslinked networks.

interactions, while demonstrating negligible affinity for aliphatic VOCs. These metrics significantly eclipsed those of commercial activated carbon. Crucially, the intrinsic hydrophobicity of the hypercrosslinked resin effectively shielded the adsorption sites from moisture interference. Under harsh 80% relative humidity, the xylene adsorption capacity retained an impressive 94.8% of its original value, in stark contrast to activated carbon, which plummeted to 48.4%. Furthermore, the material demonstrated excellent recyclability across multiple thermal regeneration cycles (120°C), thereby establishing a highly robust, waste-derived platform for practical environmental remediation (Figure 22b).

7.4 Mechanoradical Capture and Macroscopic Polymer Repair

In 2025, Hill's group reported a novel mechanochemical strategy for the efficient closed-loop recycling and macroscopic repair of PS and poly(methyl methacrylate) (PMMA) via mechanoradical capture [94]. Rather than viewing ball-milling-induced chain scission as a degradative dead-end, the team harnessed the nascent mechanoradicals by trapping them in situ with bis(butyl trithiocarbonate) under solvent-free conditions. This rapid interception quantitatively capped the severely cleaved, low-molecular-weight fragments (<20 kDa) with trithiocarbonate (TTC) end groups. Functioning as dormant macroinitiators, these TTC-terminated prepolymers underwent photoinduced iniferter polymerization, successfully driving precise chain extension to restore the molecular weight to over 150 kDa. Macroscopically, rigorous rheological assessments confirmed the complete reconstruction of topological chain entanglements and the recovery of the rubbery plateau, verifying the authentic "healing" of the bulk material properties. Remarkably, this mechanochemical repair cycle could be robustly iterated three times without performance fatigue. Furthermore, this platform offered an alternative pathway for targeted deconstruction. For PMMA, ball-milling without the TTC trapping agent directed the mechanoradicals toward disproportionation, generating terminally unsaturated chains. This defect-rich chain-end profile radically suppressed the thermal depolymerization threshold from 400°C to 220°C, facilitating a 44% monomer recovery yield under anaerobic conditions. Mechanistic investigations elucidated that radical trapping efficiency was finely dictated by the liquid-to-solid ratio, while the subsequent photochemical chain extension strictly adhered to pseudo-first-order kinetics. Ultimately, this dual-pathway paradigm elegantly bridges mechanochemistry with reversible deactivation radical polymerization, establishing a powerful blueprint for the macroscopic repair of vinyl polymers (Figure 22c).

Downloaded from https://www.cambridge.org/core. 15 Nov 2026 at 12:57:10, subject to the Cambridge Core terms of use.

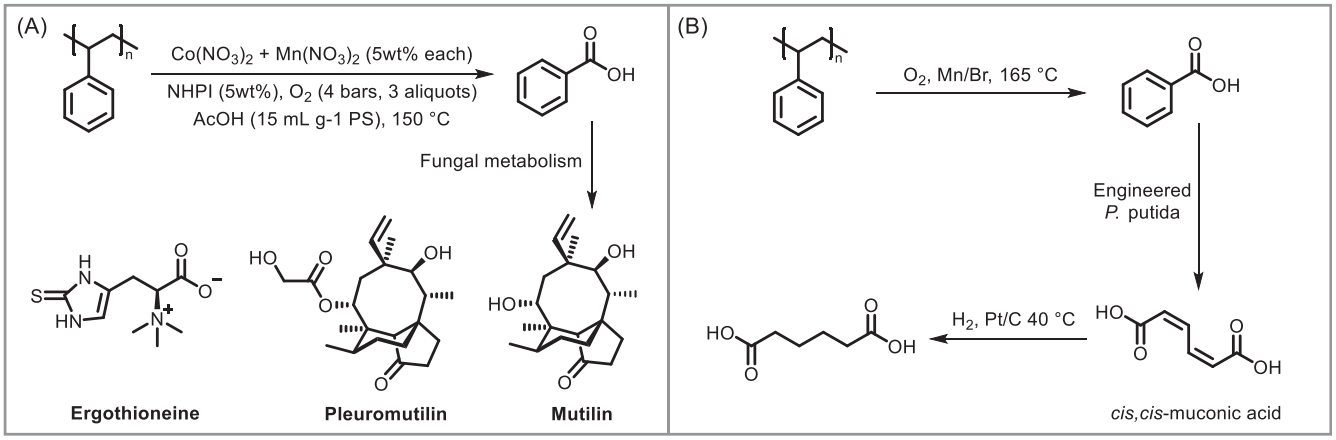


Figure 23. Materialization transformation: biologically derived and industrial platform chemicals: (a) Catalytic oxidation to benzoic acid, followed by fungal metabolism to bioactive natural products (ergothioneine, pleuromutilin, mutilin). (b) Conversion to *cis,cis*-muconic acid via engineered *Pseudomonas putida*, or to adipic acid through benzene hydrogenation/oxidation pathways.

7.5 Summary

This chapter highlights a paradigm shift in PS upcycling: from molecular-level deconstruction to macroscopic materialization. Exploiting its carbon-rich aromatic backbone, PS waste is reconfigured into high-value functional architectures, including supercapacitor electrodes, LED matrices, VOC adsorbents, and mechanochemically repaired polymers. However, industrial translation faces critical hurdles. Real-world waste impurities, coupled with the substantial logistical and preprocessing costs of post-consumer feedstocks, compromise device consistency and overall economic viability. Moreover, converting plastics into heavily crosslinked or multi-component devices poses secondary recycling challenges, risking "delayed disposal" rather than true circularity. Future innovations must inextricably integrate comprehensive LCA/TEA to ensure these material-centric approaches provide a genuinely sustainable, closed-loop destination for waste PS.

8 Biochemical Hybrid Upcycling of PS to Natural Products, Biocontrol Agents, and Bulk Chemicals

Beyond traditional chemical recycling, bio-chemical hybrid upcycling integrates the deconstructive power of chemical catalysis with the exquisite precision of synthetic biology [95,96]. Engineered microbial cell factories then process these carbon sources through a "metabolic funnel." By circumventing the structural limitations of pure chemical synthesis, this cascade seamlessly upgrades heterogeneous plastic waste into a diverse array of high-value targets, ranging from complex natural products and biocontrol agents to critical bulk chemicals.

8.1 Catalytic Oxidation Combined with Fungal Synthesis for Natural Products

In 2023, Williams's group developed a tandem chemo-biocatalytic pipeline for the upcycling of waste PS [45]. Using a Co/Mn autoxidation system with O_2, diverse post-consumer PS substrates were catalytically degraded into benzoic acid, achieving yields up to 71%. Bypassing extensive downstream purification, the crude oxidation stream was directly utilized as the sole carbon source for engineered *Aspergillus nidulans*. Integration of exogenous biosynthetic gene clusters into the AFO regulatory locus under an inducible promoter enabled the heterologous expression of three fungal natural products (ergothioneine, pleuromutilin, and mutilin), yielding fermentation titers exceeding 170 mg L^{-1}. Metabolomic analysis verified specific carbon assimilation dynamics, wherein the fungal strain exclusively metabolized benzoic acid while exhibiting physiological tolerance to unreactive PS oligomers. Expanding this platform to agricultural biocontrol, cultivation of the non-aflatoxigenic Aspergillus flavus Af36 strain on PS-derived benzoic acid induced a 5.2-fold increase in sporulation relative to glucose control media. This work validates a systemic pathway for transforming recalcitrant polyolefins into structurally complex biotherapeutics and agricultural formulations (Figure 23a).

8.2 Thermocatalytic Oxidation and Bacterial Metabolic Conversion for Adipic Acid

In 2025, Beckham's group established a tandem chemo-biological process for the conversion of waste PS into adipic acid. The protocol initiates with the thermocatalytic autoxidation of PS utilizing a Mn/Br catalyst [60]. By employing a benzoic acid/water binary solvent system, the reaction capitalizes on the high solvation capacity of benzoic acid for PS. This configuration substantially enhances substrate loading and reaction kinetics compared to conventional acetic acid systems, affording a maximum benzoic acid yield of 94%. The resulting benzoic acid stream was subsequently introduced as the carbon substrate for an engineered *Pseudomonas putida* KT2440-CJ074 strain. Harnessing the native ortho-cleavage metabolic pathway via a catechol intermediate, the microbial cell factory quantitatively funnelled benzoic acid into *cis,cis*-muconic acid. A subsequent downstream catalytic hydrogenation step reduced the muconic acid intermediate into adipic acid, thereby bridging plastic deconstruction with the synthesis of high-value nylon monomers. Furthermore, integrated TEA and LCA indicated that this hybrid process could reduce greenhouse gas emissions by 61% relative to traditional fossil-derived adipic acid synthesis, substantiating the environmental and industrial viability of this upcycling trajectory.

8.3 Photocatalytic Degradation and Microbial Conversion for Nylon-6,6 Precursors

Pushing tandem upcycling boundaries, in 2025, Wittmann's group converged dual waste streams (PS and textiles) into virgin-grade nylon-6,6. Initially, PS underwent photocatalytic oxidation into

Downloaded from https://www.cambridge.org/core. 15 Nov 2026 at 12:57:10, subject to the Cambridge Core terms of use.

Table 4. Impurity types, sources, deactivation mechanisms, and pretreatment strategies.

Impurity type	Source	Deactivation mechanism	Affected catalysts	Pretreatment
Brominated flame retardants (DBDPE)	HIPS, EPS	Irreversible poisoning (Br^- → metal sites)	Ru, Pt, Fe, Ni catalysts	Thermal debromination; solvent extraction
Inorganic fillers ($CaCO_3$, TiO_2)	Colorants, processing aids	Physical fouling; pore blockage	Zeolites; supported metals	Filtration; dissolution-precipitation
Carbonblack	Black PS products	Surface coverage; light scattering	Photocatalysts	Mechanical separation
Nitrogen-containing (caprolactam, aniline)	Co-mingled polyamides, nitrile rubbers	Reversible (aniline)/irreversible (caprolactam) binding to acid sites	Zeolites (H-ZSM–5)	Improved sorting; distillation
Polycyclic aromatic hydrocarbons	PS pyrolysis intermediates	Coke formation; pore blockage; site encapsulation	Pt/Al_2O_3; supported metals	Distillation
Polymerization retarders (benzyl-containing molecules)	Catalytic depolymerization products	Chain transfer inhibition	Repolymerization catalysts	Distillation (→ ~92% styrene)

benzoic acid [62]. Bypassing purification, this crude extract directly fed a catBC-deleted *P. putida* KT2440 chassis. Using ^{13}C metabolic flux analysis, the team identified substrate toxicity as a critical metabolic bottleneck. By implementing a dissolved oxygen (DO)-stat pulsed feeding strategy to mitigate this, they achieved a record *cis*,*cis*-muconic acid titer exceeding 65 g L^{-1}. Downstream, the fermentation intermediate was catalytically converted into a complete suite of nylon monomers. Utilizing textile-derived glucose as a fermentation co-substrate, subsequent polycondensation yielded nylon-6,6 commensurate with petrochemical standards, establishing a highly integrated paradigm for valorizing heterogeneous bulk waste (Figure 23b).

8.4 Summary

This chapter elucidates a transformative PS upcycling paradigm via a "chemical deconstruction—metabolic funnel" cascade. Advanced oxidation deconstructs the recalcitrant PS backbone into bioassimilable intermediates, predominantly benzoic acid, which are subsequently utilized by engineered microbial cell factories. This tandem approach seamlessly bridges the synthesis of complex natural products and biocontrol agents with the scalable production of bulk monomers like adipic acid. Synergizing the deconstructive power of chemical catalysis with the structural precision of synthetic biology, this pipeline circumvents the limitations of pure chemical degradation. However, mitigating the microbial toxicity of crude streams, resolving the kinetic mismatch between chemo- and biocatalysis, and integrating LCA remain critical imperatives to transition these hybrid platforms from bench-scale concepts to industrially viable realities. The sustainability merits are compelling: the PS-to-adipic acid route achieves 61% GHG reduction versus fossil-derived production. Yet challenges remain. The chemocatalytic oxidation step still requires elevated temperatures and pressurized O_2. Fermentation demands sterile conditions, nutrients, and extended residence times. A kinetic mismatch exists between relatively slow chemical deconstruction and rapid microbial metabolism, necessitating integrated process design (e.g., continuous-flow photoreactors coupled with membrane bioreactors). These bottlenecks must be resolved for industrial translation.

9 Challenges and Future Perspectives: Toward a New PS Circular Economy

Through the interdisciplinary integration of catalytic science and materials engineering, the molecular-level recycling and upcycling of PS have been pushed to new heights. Although waste PS has been demonstrated to serve as a macromolecular platform for constructing high-value-added chemicals and functional materials, a series of technological and engineering gaps must still be bridged to achieve the transition from the laboratory to industrial application. Future research can be organized around the following four core dimensions, each of which is framed around challenges that are intrinsically specific to polystyrene rather than generic to all plastics.

9.1 Substrate Heterogeneity and Catalyst Poisoning Mechanisms in Authentic PCR Streams

Transitioning from pristine model PS to authentic post-consumer recycled (PCR) streams introduces severe chemical challenges that remain largely unaddressed in academic literature. Real-world PS waste is rarely pure; high-impact polystyrene (HIPS) and expanded polystyrene (EPS) are heavily formulated with architectural additives (Table 4), most notably decabromodiphenyl ethane as a brominated flame retardant specific to PS packaging, alongside residual pentane blowing agents. During multi-energy-driven deconstruction, thermal or electro-catalytic fields inevitably induce the leaching of corrosive bromide ions from DBDPE. These halogen species possess a high affinity for active metal centers, poisoning transition-metal catalysts (e.g., Ru, Pt, or homogeneous iron porphyrins) via irreversible coordination or surface fouling. Furthermore, the volatility of trapped pentane gas alters localized pressures and interfaces in batch systems, frequently causing mass transport bottlenecks or catalyst delamination. Future research must move away from "ideal waste" imagination and prioritize the design of poisoning-resistant catalytic microenvironments capable of selectively sequestering or tolerating halogenated and aliphatic impurities intrinsic to commercial styrenic waste.

9.2 Green Energy Input Mechanisms: Expansion of Electrocatalytic and Photoelectrocatalytic Synergies

Among existing energy input modes, thermocatalysis is typically limited by harsh conditions of high temperature and pressure, while homogeneous photocatalysis faces engineering bottlenecks in scaling up. For PS in particular, the high energy demand of conventional pyrolysis (>400°C) and the thermodynamic preference for benzoic acid formation in photochemical oxidation represent two intertwined challenges that are uniquely pronounced for this aromatic polymer.

Downloaded from https://www.cambridge.org/core. 15 Nov 2026 at 12:57:10, subject to the Cambridge Core terms of use.

As a method where SET processes can be precisely controlled by adjusting the potential, electrocatalysis provides a highly promising green alternative for the degradation of inert polymers at room temperature and ambient pressure. In the future, clean electrocatalytic and photoelectrocatalytic systems should not only be widely applied to the controllable oxidative deconstruction of PS, but these reaction mechanisms are also expected to be extended to the directional conversion of engineering plastics with stronger aromatic backbones and stable ether bonds (such as polyphenylene oxide). However, for PS-specific applications, two additional considerations merit attention: (i) the insulating nature of PS necessitates the development of redox mediators or conductive supports to facilitate electron transfer from the bulk polymer to the electrode surface; and (ii) the tendency of aromatic intermediates to form coke on electrode surfaces calls for pulsed electrolysis or flow-cell designs that periodically regenerate the active interface.

9.3 Integration of In-Depth Precise Functionalization and Biochemical Hybrid Upcycling

In the high-value transformation of PS, current modification methods still face issues such as limited conversion rates and poor site selectivity; meanwhile, a ceiling often exists for the economic added value of simple chemical deconstruction products (such as benzoic acid). An effective pathway to break this limitation lies in the integration of synthetic biology. The introduction of small-molecule mixtures generated by chemical deconstruction into the "metabolic funnels" of microorganisms has been proven to be an efficient route for synthesizing high-value natural products and fine chemicals [39].

For PS in particular, the aromatic-rich nature of its degradation products presents both an opportunity and a challenge. On one hand, benzoic acid and related aromatics are readily metabolized by engineered *Pseudomonas putida* strains via the ortho-cleavage pathway [37,38]. On the other hand, the toxicity of aromatic intermediates to microbial hosts at elevated concentrations necessitates sophisticated fed-batch or DO-stat feeding strategies to maintain cell viability [37]. Future efforts should be dedicated to cultivating engineered strains with higher tolerance to aromatic toxicity, and more precise C–H bond activation and heteroatom introduction systems must be developed to adapt to and convert the complex carbon sources generated from the degradation of different batches of waste plastics. Furthermore, the kinetic mismatch between the relatively slow rates of chemical deconstruction and the rapid metabolism of engineered microbes must be resolved through integrated process design—for instance, by coupling continuous-flow photoreactors with membrane bioreactors to achieve steady-state operation.

9.4 Feedstock Logistics and the True Cost of Post-Consumer PS: Bridging Laboratory Metrics and Industrial Reality

Evaluating the genuine viability of PS upcycling demands an integrated TEA and LCA to bridge the gap between laboratory metrics and industrial reality. A pervasive blind spot in current research is the idealized assumption regarding feedstock cost. As highlighted by Liu's group, post-consumer PS is fundamentally not a "free" resource. For EPS, the ultra-low bulk density (0.01–0.02 t m^{-3}) incurs disproportionately high freight costs [97]. Moreover, municipal solid waste streams necessitate extensive, cost-intensive sorting and washing protocols. Consequently, the actual market price of PS waste in regions such as Europe can exceed €800/tonne, establishing a severe economic threshold even before any catalytic conversion begins.

Methodological challenges in cross-study LCA/TEA comparisons. Comparing LCA and TEA results across different PS upcycling studies is complicated by several methodological factors that are often overlooked. First, system boundaries vary considerably: some analyses adopt a "cradle-to-gate" perspective encompassing feedstock acquisition, pretreatment, and catalytic conversion, while others employ a narrower "gate-to-gate" scope that excludes upstream and downstream stages. The energy required for distillation of styrene monomer from pyrolysis oil, for example, accounts for approximately 39% of the total energy consumption in the recycling process, yet this is frequently underrepresented in simplified assessments. Second, the choice of functional unit profoundly influences outcomes. Products of different upcycling strategies range from bulk commodities (styrene, ~ \$1.5–2.0/kg) to specialty chemicals (benzoic acid, ~\$3–5/kg) to advanced functional materials (>\$10/kg), making mass-based comparisons inherently problematic. Third, data quality and scaling uncertainty arise from extrapolating laboratory-scale results to industrial scale; sensitivity analyses reveal that global warming potential (GWP) estimates for PS-based processes can vary by over 40% depending on assumed energy consumption and feedstock purity. Fourth, co-product allocation methods—whether by mass, economic value, or system expansion—can produce GWP differences of 30%–50% for the same process. Finally, temporal and geographical context adds further complexity, as energy mixes, labor costs, and regulatory frameworks differ substantially across regions and evolve over time. Collectively, these limitations do not invalidate LCA and TEA as tools for guiding research and development, but they necessitate that both analysts and readers approach cross-study comparisons with caution, paying close attention to underlying assumptions and system boundaries.

At the processing stage, LCA models reveal substantial variances in energy consumption across distinct upcycling trajectories. Complete depolymerization—exemplified by high-temperature pyrolysis—is highly endothermic and demands energy-intensive downstream distillation, resulting in a considerable GWP. Conversely, "skeletal preservation" strategies, such as ambient-temperature electrocatalysis or photocatalysis, theoretically mitigate these energy penalties by circumventing the high activation barrier of total C–C backbone cleavage. In practice, however, this environmental advantage is frequently offset by severe operational bottlenecks. Most homogeneous catalytic protocols rely on large volumes of hazardous or high-boiling-point solvents, and LCA consistently shows that the energy required for solvent recovery, product isolation, and catalyst separation often negates the thermodynamic savings achieved under mild conditions.

To break this thermodynamic and economic deadlock, inspiration can be drawn from recent macro-scale demonstrations in other polyolefin upcycling. For instance, an oxygen-mediated tandem strategy was recently developed to drive the endothermic aromatization of polyethylene by selectively oxidizing in-situ generated hydrogen—a kinetic coupling principle that could be adapted to PS systems where similar thermodynamic trade-offs govern product selectivity. This kinetic coupling successfully shifted the thermodynamic equilibrium, achieving an unprecedented 78 mol% aromatic selectivity under mild conditions without relying on massive solvent volumes. Importantly, pilot-scale demonstrations (500 g) and subsequent TEA revealed a highly competitive minimum selling price of \$1.05/kg. This underscores

Downloaded from https://www.cambridge.org/core. 15 Nov 2026 at 12:57:10, subject to the Cambridge Core terms of use.

that intelligently coupling endothermic and exothermic cascades is a viable engineering route to offset scaling costs [98].

To translate molecular-level upcycling into tangible environmental and economic benefits, future paradigms must simultaneously address these front-end (feedstock logistics) and back-end (downstream separation) bottlenecks. From a technological standpoint, priority should be given to solvent-free or high-solid paradigms (e.g., mechanochemistry, liquid-assisted grinding), the development of robust heterogeneous catalysts to preclude metal leaching, and tandem reaction cascades that minimize intermediate purification steps. Economically, alternative upcycling strategies should strategically bypass conventional multistep synthesis to deliver high-value pharmaceutical scaffolds and fine chemical building blocks. Only by generating a substantial economic delta through premium products can the process offset both the unavoidable logistical burdens of waste procurement and the capital costs of industrial scale-up.

Open peer review. To view the open peer review materials for this article, please visit http://doi.org/10.1017/S2978169826000021.

Declaration of Generative AI and AI-Assisted Technologies in the Writing Process. During the preparation of this work, the authors used DeepSeek (DeepSeek-V3, accessed via https://www.deepseek.com) in order to improve clarity, grammar, and overall flow of the manuscript. After using this tool, the authors reviewed and edited the content as needed and take full responsibility for the content of the published article.

Author Contributions. Conceptualization: X.J. and H.S.; Investigation: H.S. and X.Z.; Methodology: X.J.; Project administration: X.J.; Supervision: X.J.; Writing-original draft: H.S.; Writing-review and editing: X.J., H.S., and X.Z.

Financial Support. The authors are grateful for financial support from the National Natural Science Foundation of China (22125103).

Competing Interests. The authors declare that they have no competing interests.

Data Availability Statement. Data are available upon request.

References

[1] J. C. Capricho, K. Prasad, N. Hameed, M. Nikzad and N. Salim, 'Upcycling polystyrene'. *Polymers*, 14(22): (2022), 5010. https://doi.org/10.3390/polym14225010.

[2] C. Signoret, M. Edo, D. Lafon et al., 'Degradation of styrenic plastics during recycling: impact of reprocessing photodegraded material on aspect and mechanical properties'. *Journal of Polymers and the Environment*, 28(8): (2020), 2055–2077. https://doi.org/10.1007/s10924-020-01741-8.

[3] R. Cao, D. Xiao, M. Wang, Y. Gao and D. Ma, 'Solar-driven photocatalysis for recycling and upcycling plastics'. *Applied Catalysis B: Environment and Energy*, 341: (2024), 123357. https://doi.org/10.1016/j.apcatb.2023.123357.

[4] C. Jehanno, J. W. Alty, M. Roosen et al., 'Critical advances and future opportunities in upcycling commodity polymers'. *Nature*, 603(7903): (2022), 803–814. https://doi.org/10.1038/s41586-021-04350-0.

[5] L. D. Ellis, N. A. Rorrer, K. P. Sullivan et al., 'Chemical and biological catalysis for plastics recycling and upcycling'. *Nature Catalysis*, 4(7): (2021), 539–556. https://doi.org/10.1038/s41929-021-00648-4.

[6] S. Billiet and S. R. Trenor, '100th anniversary of macromolecular science viewpoint: needs for plastics packaging circularity'. *ACS Macro Letters*, 9(9): (2020), 1376–1390. https://doi.org/10.1021/acsmacrolett.0c00437.

[7] J. P. Lange, 'Managing plastic waste—sorting, recycling, disposal, and product redesign'. *ACS Sustainable Chemistry & Engineering*, 9(47): (2021), 15722–15738. https://doi.org/10.1021/acssuschemeng.1c05013.

[8] J. W. Summers, 'The melting temperature (or not melting) of poly(vinyl chloride)'. *Journal of Vinyl and Additive Technology*, 14(3): (2008), 105–109. https://doi.org/10.1002/vnl.20151.

[9] D. E. MacArthur, 'Beyond plastic waste'. *Science*, 358(6365): (2017), 843. https://doi.org/10.1126/science.aao6749.

[10] J. M. Garcia and M. L. Robertson, 'The future of plastics recycling'. *Science*, 358(6365): (2017), 870–872. https://doi.org/10.1126/science.aaq0324.

[11] D. K. Schneiderman and M. A. Hillmyer, '50th anniversary perspective, there is a great future in sustainable polymers'. *Macromolecules*, 50(10): (2017), 3733–3749. https://doi.org/10.1021/acs.macromol.7b00293.

[12] I. Vollmer, M. J. F. Jenks, M. C. P. Roelands et al., 'Beyond mechanical recycling: giving new life to plastic waste'. *Angewandte Chemie International Edition*, 59(36): (2020), 15402–15423. https://doi.org/10.1002/anie.201915651.

[13] R. A. Sheldon and M. Norton, 'Green chemistry and the plastic pollution challenge: towards a circular economy'. *Green Chemistry.*, 22(19): (2020), 6310–6322. https://doi.org/10.1039/D0GC02630A.

[14] G. W. Coates and Y. D. Y. L. Getzler, 'Chemical recycling to monomer for an ideal, circular polymer economy'. *Nature Reviews Materials*, 5(7): (2020), 501–516. https://doi.org/10.1038/s41578-020-0190-4.

[15] J. Savoldelli, D. Tomback and H. Savoldelli, 'Breaking down polystyrene through the application of a two-step thermal degradation and bacterial method to produce usable byproducts'. *Waste Management*, 60: (2017), 123–126. https://doi.org/10.1016/j.wasman.2016.04.017.

[16] D. Baek, D. J. Walsh, J. B. Gerken et al., 'Conversion of polystyrene to terephthalic acid via sequential acetylation and Mn/Br-catalyzed autoxidation'. *ACS Catalysis*, 15(18): (2025), 16421–16426. https://doi.org/10.1021/acscatal.5c04744.

[17] A. L. De Abreu, D. Taton and D. M. Bassani, 'Reassessing the photochemical upcycling of polystyrene using acridinium salts'. *Angewandte Chemie International Edition*, 64(6): (2025), e202418680. https://doi.org/10.1002/anie.202418680.

[18] H. Jiang, E. A. Medina and E. E. Stache, 'Upcycling poly(vinyl chloride) and polystyrene plastics using photothermal conversion'. *Journal of the American Chemical Society*, 147(3): (2025), 2822–2828. https://doi.org/10.1021/jacs.4c16145.

[19] A. Chamas, H. Moon, J. Zheng et al., 'Degradation rates of plastics in the environment'. *ACS Sustainable Chemistry & Engineering*, 8(9): (2020), 3494–3511. https://doi.org/10.1021/acssuschemeng.9b06635.

[20] Y. Miao, A. Jouanne and A. Yokochi, 'Current technologies in depolymerization process and the road ahead'. *Polymers*, 13(3): (2021), 449. https://doi.org/10.3390/polym13030449.

[21] G. Faraca and T. Astrup, 'Plastic waste from recycling centres: characterisation and evaluation of plastic recyclability'. *Waste Management*, 95: (2019), 388–398. https://doi.org/10.1016/j.wasman.2019.06.038.

[22] K. Ragaert, L. Delva and K. Van Geem, 'Mechanical and chemical recycling of solid plastic waste'. *Waste Management*, 69: (2017), 24–58. https://doi.org/10.1016/j.wasman.2017.07.044.

[23] L. Wimberger, G. Ng and C. Boyer, 'Light-driven polymer recycling to monomers and small molecules'. *Nature Communications*, 15(1): (2024), 2510. https://doi.org/10.1038/s41467-024-46656-3.

[24] M. Hong and E. Y. X. Chen, 'Chemically recyclable polymers: a circular economy approach to sustainability'. *Green Chemistry*, 19(16): (2017), 3692–3706. https://doi.org/10.1039/C7GC01496A.

[25] S. Kumar, E. Singh, R. Mishra, A. Kumar and S. Caucci, 'Utilization of plastic wastes for sustainable environmental management: a review'. *ChemSusChem*, 14(19): (2021), 3985–4006. https://doi.org/10.1002/cssc.202101631.

[26] I. A. Ignatyev, W. Thielemans and B. V. Beke, 'Recycling of polymers: a review'. *ChemSusChem*, 7(6): (2014), 1579–1593. https://doi.org/10.1002/cssc.201300898.

[27] ASTM, 'ASTM D7209-06 Standard Guide for Waste Reduction, Resource Recovery, and Use of Recycled Polymeric Materials and Products'. In *ASTM International* (Conshohocken, PA: West, 2006).

[28] ISO, *ISO 15270:2008 Plastics—Guidelines for the Recovery and Recycling of Plastics Waste* (Geneva, Switzerland: International Organization for Standardization, 2008).

[29] OECD, *Global Plastics Outlook: Economic Drivers, Environmental Impacts and Policy Options* (Paris, France: OECD Publishing, 2022).

Downloaded from https://www.cambridge.org/core. 15 Nov 2026 at 12:57:10, subject to the Cambridge Core terms of use.

[30] V. Tournier, S. Duquesne, F. Guillamot et al., 'Enzymes' power for plastics degradation'. *Chemical Reviews*, 123(9): (2023), 5612–5701. https://doi.org/10.1021/acs.chemrev.2c00644.

[31] S. J. Liu, J. J. Yang, W. L. Huang et al., 'Dissolved organic matter inhibit the degradation process of polystyrene nanoplastic under utraviolet light'. *Water Research*, 292: (2026), 125341. https://doi.org/10.1016/j.watres.2026.125341.

[32] C. Marquez, C. Martin, N. Linares and D. de Vos, 'Catalytic routes towards polystyrene recycling'. *Materials Horizons*, 10(5): (2023), 1625–1640. https://doi.org/10.1039/D2MH01215D.

[33] A. Rizzo and G. I. Peterson, 'Progress toward sustainable polymer technologies with ball-mill grinding'. *Progress in Polymer Science*, 159: (2024), 101900. https://doi.org/10.1016/j.progpolymsci.2024.101900.

[34] D. Xu, H. Wang, K. Zhang et al., 'Photocatalytic waste polystyrene plastic conversion: reaction mechanism and catalyst design'. *Environmental Science & Technology*, 59(31): (2025), 16112–16129. https://doi.org/10.1021/acs.est.5c07160.

[35] B. Gu, C. Li and X. Jiang, 'Chemical upcycling of polyphenylene sulfide at room temperature'. *Advanced Science*, 13(22): (2026), e19090. https://doi.org/10.1002/advs.202519090.

[36] R. Huang, Y. Zhao, C. Li, D. Li and X. Jiang, 'Photocatalytic upcycling of polysulfones at ambient conditions'. *Nature Sustainability*, 8(7): (2025), 818–826. https://doi.org/10.1038/s41893-025-01569-x.

[37] L. Ji, J. Meng, C. Li, M. Wang and X. Jiang, 'From polyester plastics to diverse monomers via low-energy upcycling'. *Advanced Science*, 11(25): (2024), e2403002. https://doi.org/10.1002/advs.202403002.

[38] C. Li, J. Meng and X. Jiang, 'Photocatalyzed relay cleavage for the upcycling of gem-dimethyl-type plastics'. *Science Bulletin*, 71(9): (2026), 2230–2239. https://doi.org/10.1016/j.scib.2026.04.009.

[39] J. Meng, Y. Zhou, D. Li and X. Jiang, 'Degradation of plastic wastes to commercial chemicals and monomers under visible light'. *Science Bulletin*, 68(14): (2023), 1522–1530. https://doi.org/10.1016/j.scib.2023.06.024.

[40] B. C. Vance, S. Najmi and D. G. Vlachos, 'Polystyrene hydrogenolysis to high-quality lubricants using Ni/SiO_2'. *ACS Catalysis*, 14(7): (2024), 5389–5402. https://doi.org/10.1021/acscatal.3c05900.

[41] J. Wang, Z. Zhang, Y. Zhang et al., 'Breaking the yield-selectivity trade-off in polystyrene waste valorization via tandem depolymerization and hydrogenolysis'. *Nature Nanotechnology*, 21(1): (2026), 87–94. https://doi.org/10.1038/s41565-025-02069-x.

[42] M. C. Wang, J. Li, A. Zelina, B. Pepper and J. Wang, 'Mechanochemical degradation of polystyrene into benzene for recycling and upcycling'. *Angewandte Chemie International Edition*, 64(41): (2025), e202512687. https://doi.org/10.1002/anie.202512687.

[43] S. Oh, H. Jiang, L. H. Kugelmass and E. E. Stache, 'Recycling of post-consumer waste polystyrene using commercial plastic additives'. *ACS Central Science*, 11(1): (2025), 57–65. https://doi.org/10.1021/acscentsci.4c01317.

[44] G. Zhang, Z. Zhang, R. Zeng. 'Photoinduced $FeCl_3$-catalyzed alkyl aromatics oxidation toward degradation of polystyrene at room temperature†'. *Chinese Journal of Chemistry*, 39(12): (2021), 3225–3230. https://doi.org/10.1002/cjoc.202100420.

[45] C. Rabot, Y. Chen, S. Y. Lin et al., 'Polystyrene upcycling into fungal natural products and a biocontrol agent'. *Journal of the American Chemical Society*, 145(9): (2023), 5222–5230. https://doi.org/10.1021/jacs.2c12285.

[46] H. Lee, Y. Kim, H. Ryou et al., 'Upcycling post-consumer polystyrene waste into liquid organic hydrogen carriers'. *ACS Catalysis*, 15(15): (2025), 13243–13259. https://doi.org/10.1021/acscatal.5c00533.

[47] S. Oh, N. Ayala, L. J. Broadbelt et al., 'Mechanistic interpretation of base-catalyzed depolymerization of polystyrene'. *Catalysis Today*, 55(1-2): (2000), 161–171. https://doi.org/10.1016/S0920-5861(99)00235-7.

[48] A. Thigale, C. Trant, J. Ahn et al., 'Superacid-assisted degradation of polystyrene'. *Macromolecules*, 56(13): (2023), 5117–5126. https://doi.org/10.1021/acs.macromol.3c00602.

[49] C. Qin, J. Liu, H. Hu et al., 'Upcycling of polystyrene to styrene via a Lewis Acid–Base synergistic catalyst ZAS-16(Vo) in aromatic solvents'. *ACS Sustainable Chem. Eng.*, 14(23): (2026), 10658–10668. https://doi.org/10.1021/acssuschemeng.6c02655.

[50] K. Parkatzidis, H. S. Wang and A. Anastasaki, 'Photocatalytic upcycling and depolymerization of vinyl polymers'. *Angewandte Chemie International Edition*, 63(19): (2024), e202402436. https://doi.org/10.1002/anie.202402436.

[51] R. Zeng, C. Ke, S. Wang et al., '$FeCl_3$-catalyzed aerobic oxidative degradation of polystyrene to benzoic acid: scope and mechanism'. *Synlett*, 35: (2023), 1175–1179.

[52] S. Oh and E. E. Stache, 'Chemical upcycling of commercial polystyrene via catalyst-controlled photooxidation'. *Journal of the American Chemical Society*, 144(13): (2022), 5745–5749. https://doi.org/10.1021/jacs.2c01411.

[53] S. Oh and E. E. Stache, 'Mechanistic insights enable divergent product selectivity in catalyst-controlled photooxidative degradation of polystyrene'. *ACS Catalysis*, 13(16): (2023), 10968–10975. https://doi.org/10.1021/acscatal.3c02516.

[54] Y. Yu, Y. Zhu, J. Liu et al., 'Highly selective aerobic oxidation of polystyrene to benzoic acid catalyzed by nitrogen dioxide'. *Science Bulletin*, 70(15): (2025), 2463–2472. https://doi.org/10.1016/j.scib.2025.05.034.

[55] M. Hourtoule, P. Skumial, S. Trienes et al., 'Synergistic effects of electricity and light for efficient iron-catalyzed recycling of polystyrene waste'. *Angewandte Chemie International Edition*, 65(7): (2026), e19237. https://doi.org/10.1002/anie.202519237.

[56] A. Ong, Z. Zhang, J. Y. Teo, Y. H. Lee and J. Y. C. Lim, 'Upcycling of polystyrene to 1,2-disubstituted oxygenated aromatics through backbone rearrangement and oxidation reactions'. *Angewandte Chemie International Edition*, 64(44): (2025), e202515072. https://doi.org/10.1002/anie.202515072.

[57] B. Zhao, Z. Hu, Y. Sun et al., 'Selective upcycling of polyolefins into high-value nitrogenated chemicals'. *Journal of the American Chemical Society*, 146(42): (2024), 28605–28611. https://doi.org/10.1021/jacs.4c07965.

[58] S. E. Lewis, B. E. Wilhelmy and F. A. Leibfarth, 'Upcycling aromatic polymers through C-H fluoroalkylation'. *Chemical Science*, 10(25): (2019), 6270–6277. https://doi.org/10.1039/C9SC01425J.

[59] C. Ma, X. Liu, J. Min et al., 'Sustainable recycling of waste polystyrene into hierarchical porous carbon nanosheets with potential applications in supercapacitors'. *Nanotechnology*, 31(3): (2020), 035402. https://doi.org/10.1088/1361-6528/ab475f.

[60] H. Moon, J. S. Des Veaux, E. C. Van Roijen et al., 'Upcycling waste polystyrene to adipic acid through a hybrid chemical and biological process'. *Nature Communications*, 16(1): (2025), 9543. https://doi.org/10.1038/s41467-025-64561-1.

[61] Z. Huang, M. Shanmugam, Z. Liu et al., 'Chemical recycling of polystyrene to valuable chemicals via selective acid-catalyzed aerobic oxidation under visible light'. *Journal of the American Chemical Society*, 144(14): (2022), 6532–6542. https://doi.org/10.1021/jacs.2c01410.

[62] M. Kohlstedt, F. Weiland, S. Pearson et al., 'Biological upcycling of polystyrene into ready-to-use plastic monomers and plastics using metabolically engineered pseudomonas putida'. *Chemical Engineering Journal*, 524: (2025), 168431. https://doi.org/10.1016/j.cej.2025.168431.

[63] T. Li, A. Vijeta, C. Casadevall et al., 'Bridging plastic recycling and organic catalysis: photocatalytic deconstruction of polystyrene via a C-H oxidation pathway'. *ACS Catalysis*, 12(14): (2022), 8155–8163. https://doi.org/10.1021/acscatal.2c02292.

[64] N. F. Nikitas, E. Skolia, P. L. Gkizis, I. Triandafillidi and C. G. Kokotos, 'Photochemical aerobic upcycling of polystyrene plastics to commodity chemicals using anthraquinone as the photocatalyst'. *Green Chemistry*, 25(12): (2023), 4750–4759. https://doi.org/10.1039/D3GC00986F.

[65] S. Zhang, J. Wang, D. Su and X. Xiao, 'Facile visible-light upcycling of diverse waste plastics using a single organocatalyst with minimal loadings'. *Nature Communications*, 16(1): (2025), 4188. https://doi.org/10.1038/s41467-025-59540-5.

[66] Y. Qin, T. Zhang, H. Y. V. Ching, G. S. Raman and S. das, 'Integrated strategy for the synthesis of aromatic building blocks via upcycling of real-life plastic wastes'. *Chem*, 8(9): (2022), 2472–2484. https://doi.org/10.1016/j.chempr.2022.06.002.

[67] C. Li, X. Y. Kong, M. Lyu et al., 'Upcycling of non-biodegradable plastics by base metal photocatalysis'. *Chem*, 9(9): (2023), 2683–2700. https://doi.org/10.1016/j.chempr.2023.07.008.

Downloaded from https://www.cambridge.org/core. 15 Nov 2026 at 12:57:10, subject to the Cambridge Core terms of use.

[68] D. Yang, J. Li, M. Xiao et al., 'Atomically dispersed metal catalysts towards nitrogen reduction for ammonia: from homogeneous to heterogeneous'. *Chemical Engineering Journal*, 468: (2023), 143776. https://doi.org/10.1016/j.cej.2023.143776.

[69] O. A. Zelekew, Z. Wang, Y. Gu and Y. N. Wu, 'Recent progress on photoactive heterogeneous photocatalysts for the degradation of per-and polyfluoroalkyl substances (PFAS): mechanisms, DFT calculations, limitations, and future prospects'. *Journal of Environmental Chemical Engineering*, 12(5): (2024), 113323. https://doi.org/10.1016/j.jece.2024.113323.

[70] R. Cao, M. Q. Zhang, C. Hu et al., 'Catalytic oxidation of polystyrene to aromatic oxygenates over a graphitic carbon nitride catalyst'. *Nature Communications*, 13(1): (2022), 4809. https://doi.org/10.1038/s41467-022-32510-x.

[71] Z. Peng, R. Chen and H. Li, 'Heterogeneous photocatalytic oxidative cleavage of polystyrene to aromatics at room temperature'. *ACS Sustainable Chemistry & Engineering*, 11(29): (2023), 10688–10697. https://doi.org/10.1021/acssuschemeng.3c01282.

[72] Z. M. Saeed, T. Jadhav, R. Mathew et al., 'Heterogeneous iron-doped covalent triazine framework for the efficient photocatalytic upcycling of polystyrene waste to valuable aromatics under ambient conditions'. *Chemical Engineering Journal*, 537: (2026), 175007. https://doi.org/10.1016/j.cej.2026.175007.

[73] A. Ong, J. Y. Q. Teo, Z. Feng, T. T. Y. Tan and J. Y. C. Lim, 'Organocatalytic aerobic oxidative degradation of polystyrene to aromatic acids'. *ACS Sustainable Chemistry & Engineering*, 11(34): (2023), 12514–12522. https://doi.org/10.1021/acssuschemeng.3c01387.

[74] B. Zhao, H. Tan, J. Yang et al., 'Catalytic conversion of mixed polyolefins under mild atmospheric pressure'. *The Innovation*, 5(2): (2024), 100586. https://doi.org/10.1016/j.xinn.2024.100586.

[75] S. Zhang, M. Chu, Q. Zhang et al., 'Spent battery-to-catalyst: asymmetric Mn−O motifs boost oxygen activation for upgrading polystyrene to aromatic oxygenates'. *ACS Nano*, 20(4): (2026), 3724–3734. https://doi.org/10.1021/acsnano.5c18041.

[76] D. Baek, A. J. Al Abdulghani, D. J. Walsh et al., 'Can the hock process be used to produce phenol from polystyrene?'. *Journal of the American Chemical Society*, 147(10): (2025), 8687–8694. https://doi.org/10.1021/jacs.4c18143.

[77] S. F. He, T. Xu, Q. Wan et al., 'Divergent upcycling of polystyrene into phenol and hydroquinone derivatives by photocatalysis and electrocatalysis'. *Angewandte Chemie International Edition*, 64(34): (2025), e202508166. https://doi.org/10.1002/anie.202508166.

[78] H. Jiang, S. Oh, E. E. Stache et al., 'Photooxidative upcycling of post-consumer polystyrene plastics into phenol using eosin Y'. *ACS Catalysis*, 16: (2026), 12135–12140. https://doi.org/10.1021/acscatal.6c01400.

[79] N. S. Giakoumakis, C. Marquez, R. de Oliveira-Silva, D. Sakellariou and D. E. de Vos, 'Upcycling of polystyrene to aromatic polyacids by tandem friedel-crafts and oxidation reactions'. *Journal of the American Chemical Society*, 146(50): (2024), 34753–34762. https://doi.org/10.1021/jacs.4c13265.

[80] J. Jia, J. Liu, Z. Wang et al., 'Photoinduced inverse vulcanization'. *Nature Chemistry*, 14(11): (2022), 1249–1257. https://doi.org/10.1038/s41557-022-01049-1.

[81] H. Song, J. Meng and X. Jiang, 'Sulfur-containing sustainable polymers: synthetic pathways, degradation mechanisms, and multifunctional applications'. *National Science Review*, 12(12): (2025), nwaf475. https://doi.org/10.1093/nsr/nwaf475.

[82] N. E. Munyaneza, C. Posada, Z. Xu et al., 'A generic platform for upcycling polystyrene to aryl ketones and organosulfur compounds'. *Angewandte Chemie International Edition*, 62(36): (2023), e202307042. https://doi.org/10.1002/anie.202307042.

[83] Y. Liu, H. Liu, Z. H. Wang et al., 'Solar-driven upcycling of polystyrene enabled by elemental sulfur'. *Journal of the American Chemical Society*, 148(9): (2026), 10193–10204. https://doi.org/10.1021/jacs.6c01318.

[84] B. Dou, Y. Xu and J. Wang, 'Gold-catalyzed precise bromination of polystyrene'. *Journal of the American Chemical Society*, 145(18): (2023), 10422–10430. https://doi.org/10.1021/jacs.3c03069.

[85] R. Liu, C. Lin, Y. Zou et al., 'Post-polymerization modification of polystyrene through Mn-catalyzed phosphorylation of aromatic C(sp^2)–H bonds'. *ACS Applied Polymer Materials*, 6(18): (2024), 11633–11640. https://doi.org/10.1021/acsapm.4c02382.

[86] R. Ebenbauer, T. A. Møller, J. Bjørn et al., 'CO_2 capture with catalytically upcycled polystyrene plastics'. *Chem Circularity*, 1(1): (2026), 100027. https://doi.org/10.1016/j.checir.2026.100027.

[87] Z. Siddiqi and D. Sarlah, 'Electrochemical Dearomatization of commodity polymers'. *Journal of the American Chemical Society*, 143(50): (2021), 21264–21269. https://doi.org/10.1021/jacs.1c11546.

[88] R. A. Naumann, M. A. Clerk, R. E. Hernandez and N. A. Romero, 'Electrochemical C-H functionalization and defunctionalization of polystyrene'. *Journal of the American Chemical Society*, 147(41): (2025), 37272–37279. https://doi.org/10.1021/jacs.5c10490.

[89] N. Ohn and J. G. Kim, 'Mechanochemical post-polymerization modification: solvent-free solid-state synthesis of functional polymers'. *ACS Macro Letters*, 7(5): (2018), 561–565. https://doi.org/10.1021/acsmacrolett.8b00171.

[90] M. E. Skala, S. M. Zeitler and M. R. Golder, 'Liquid-assisted grinding enables a direct mechanochemical functionalization of polystyrene waste'. *Chemical Science*, 15(28): (2024), 10900–10907. https://doi.org/10.1039/D4SC03362K.

[91] G. Kim, B. Park, N. Kim et al., 'Waste polystyrene upcycling via the birch reduction with ball-mill grinding'. *Nature Communications*, 16(1): (2025), 5924. https://doi.org/10.1038/s41467-025-61119-z.

[92] H. Su, H. Lin, P. Li et al., 'Conversion of waste expanded polystyrene into blue-emitting polymer film for light-emitting diode applications'. *Polymers*, 15(24): (2023), 4693. https://doi.org/10.3390/polym15244693.

[93] A. Varyambath, C.-P. Hu, H. Chen et al., 'Upcycling of expanded polystyrene wastes into reusable high-performance volatile organic compound adsorbents'. *ACS Sustainable Resource Management*, 2(5): (2025), 815–824. https://doi.org/10.1021/acssusresmgt.5c00052.

[94] A. R. Cunningham, G. C. Wilusz, O. A. Lee, J. C. Estock and M. R. Hill, 'Effective recycling pathways of commodity polymers enabled by mechanoradical capture'. *Journal of the American Chemical Society*, 147(46): (2025), 42549–42558. https://doi.org/10.1021/jacs.5c13585.

[95] J. M. Borrero-de Acuna, I. Gutierrez-Urrutia, C. Hidalgo-Dumont et al., 'Channelling carbon flux through the meta-cleavage route for improved poly(3-hydroxyalkanoate) production from benzoate and lignin-based aromatics in pseudomonas putida H'. *Microbial Biotechnology*, 14(6): (2021), 2385–2402. https://doi.org/10.1111/1751-7915.13705.

[96] P. Dvorak, P. I. Nikel, J. Damborsky et al., 'Bioremediation 3.0: engineering pollutant-removing bacteria in the times of systemic biology'. *Biotechnology Advances*, 35(7): (2017), 845–866. https://doi.org/10.1016/j.biotechadv.2017.08.001.

[97] Z. Xu, D. Sun, J. Xu et al., 'Progress and challenges in polystyrene recycling and upcycling'. *ChemSusChem*, 17(17): (2024), e202400474. https://doi.org/10.1002/cssc.202400474.

[98] S. Li, W. Tu, W. Zhang et al., 'Oxygen-mediated tandem polyethylene upcycling for selective aromatic synthesis'. *National Science Review*, 13(12): (2026), nwag207. https://doi.org/10.1093/nsr/nwag207.

Downloaded from https://www.cambridge.org/core. 15 Nov 2026 at 12:57:10, subject to the Cambridge Core terms of use.